

The responses to the comments of the referee in our direct reply (shown below) and within the revised manuscript (see marked copy) are provided. The pages and lines indicated below correspond to those in the marked copy.

Response to Referee 1 (Referee's comments are italicized)

1. Referee's comment: *“Although several caveats have been introduced noting that the peak assignments are speculative, the same interpretations follow. The speculation is ok, but there should be no further quantification or interpretation based upon that. Without further justification, the organic acids should not be identified as a single compound and their abundance should not be interpreted. Instead, please show them as masses, or as a sum of compounds. The figures may be very misleading by showing individual compounds as mixing ratios. If molecule names are used, then some simple tests ought to be performed to inform the identification of the masses. Can an HR-TOF be used with SF₆⁻ in a similar environment to see which compounds dominate? That would be far more powerful than the comparison with WSOCg.”*

Author response: We will agree that that with the exception of formic, acetic, oxalic and propionic acids, we do not have sufficient evidence to justify the assignment of other the organic acids. Hence, we will refer to organic acids with m/z 75, 87, 101, 103, 117 and 131 by their ion masses.

We are confident in our peak assignment of formic, acetic and propionic acids because the SF₆⁻ ion chemistry is selective to acidic species and these three acids do not have organic acid isomers and isobaric species. In addition, we are confident in our peak assignment of oxalic acid because the estimated gas-phase oxalic acid concentration make sense relative to its particle concentrations, which were also measured during the study. As explained in Nah et al. (2018), the gas-particle ratios of the organic acids depend of their thermodynamic conditions, which are dependent on the acid's physicochemical properties, ambient temperature, particle water and pH. In the case of oxalic acid, the measured gas-particle partitioning ratios are in good agreement with their corresponding thermodynamic predictions, thus indicating that our assignment of the m/z 89 ion to oxalic acid is reasonable.

The manuscript has been revised as follows:

Page 18 line 546: “3.2.3. Larger organic acids

In addition to formic and acetic acid, eight other ions were monitored during the field study: m/z 73, 75, 87, 89, 101, 103, 117 and 131. These ions were chosen as they had significant signals when ambient air was sampled and were not obviously formed from SF₆⁻ reaction with water vapor or O₃. Since the CIMS utilized in this study only had unit mass resolution, these ions are the sum of all organic acid isomers and isobaric organic acids of the same molecular weight as well as other product ions from species that might react with SF₆⁻. We will refer to organic acids with m/z 75, 87, 101, 103, 117 and 131 by their ion masses. We assign the m/z 73 ion as the X⁻ ion of propionic acid because it does not have organic acid isomers and isobaric species at that m/z. In addition, real-time ion chromatography measurements of aerosol composition performed during the field study demonstrated the presence of particulate oxalic acid (Nah et al., 2018). For this reason, we assign the m/z 89 ion as the X⁻ ion of oxalic acid. As shown in Nah et al. (2018), the gas-particle ratios of the

organic acids depend of their thermodynamic conditions, which are dependent on the acid's physicochemical properties, ambient temperature, particle water and pH. Since the measured gas-particle partitioning ratios of oxalic acid (calculated using the CIMS and ion chromatography measurements) are in good agreement with their corresponding thermodynamic predictions (Nah et al., 2018), this indicated that our assignment of the m/z 89 ion to oxalic acid is reasonable. In addition, the high sensitivity of SF_6^- to oxalic acid also helps limit interferences due to other acids. Particulate formic acid and acetic acid were also detected by ion chromatography during the field study, but were at much lower concentrations relative to the gas phase (Nah et al., 2018).

Figures 5 and S5 show the time series and diurnal profiles of oxalic and propionic acids and organic acids with ions m/z 75, 87, 101, 103, 117 and 131 measured during the field study. These organic acids displayed very similar day-to-day variability as formic and acetic acids, with higher concentrations (or ion signals) being measured on warm and sunny days. The diurnal profiles of all the measured organic acids have similar diurnal trends, with their concentrations (or ion signals) reaching a maximum between 17:30 and 19:30 and rapidly decreasing after sunset.”

Page 24 line 798: “The SF_6^- CIMS method was deployed for measurements of gas phase organic acids in a mixed forest-agricultural area in Yorkville, Georgia from Sept to Oct 2016. The organic acids measured in the field study were formic, acetic, propionic and oxalic acids.”

Reference:

Nah, T., Guo, H., Sullivan, A. P., Chen, Y., Tanner, D. J., Nenes, A., Russell, A., Ng, N. L., Huey, L. G., and Weber, R. J.: Characterization of Aerosol Composition, Aerosol Acidity and Organic Acid Partitioning at an Agriculture-intensive Rural Southeastern U.S. Site, *Atmos. Chem. Phys. Discuss.*, in review, 10.5194/acp-2018-373, 2018.

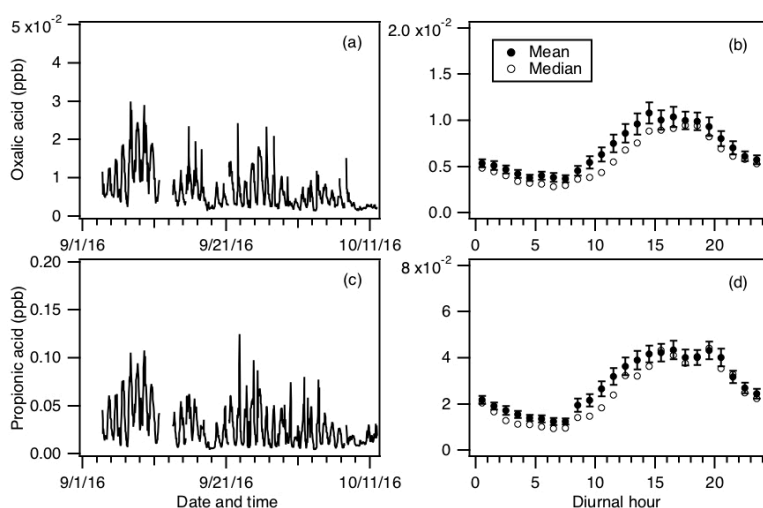


Figure 5: Time series of concentrations of (a) oxalic and (c) propionic acids measured during the field study. All the data are displayed as 1-hour averages. Their corresponding diurnal profiles are shown in (b) and (d), respectively. The diurnal profile concentrations represent averages in 1-hour intervals and the standard errors are plotted as error bars.

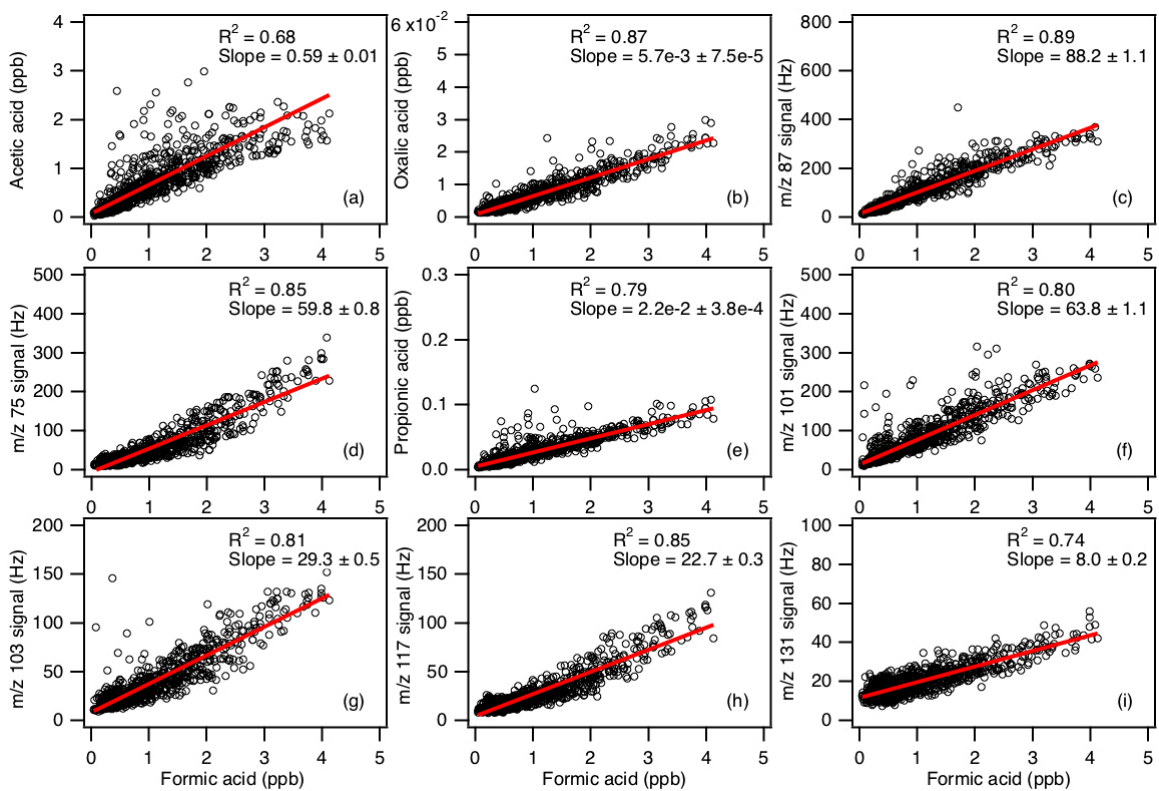


Figure 7: Scatter plots of concentrations (or ion signals) of the measured organic acids with formic acid concentration. All the data are displayed as 1-hour averages. Red lines shown are linear fits to the data.

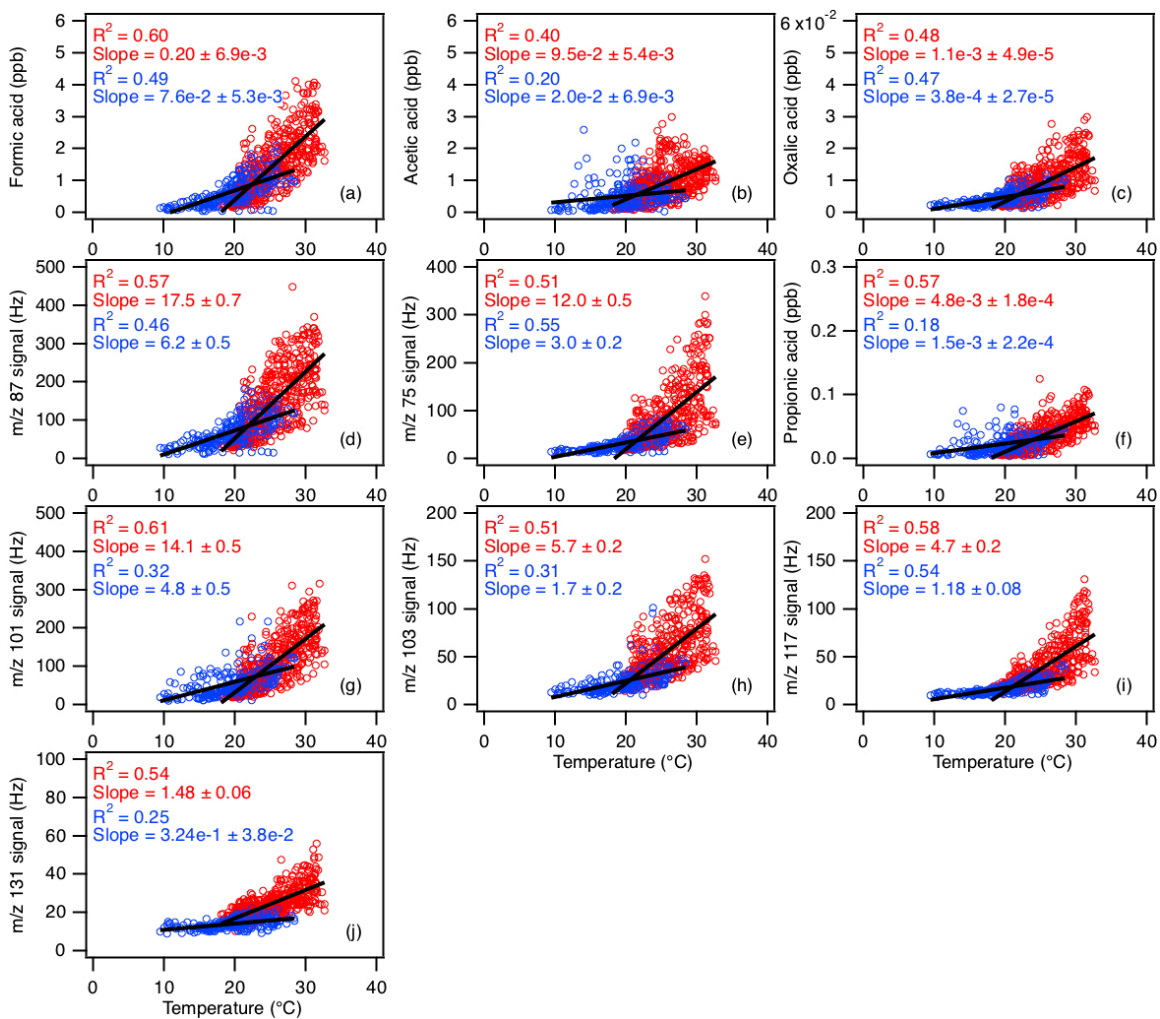


Figure 8: Scatter plots of concentrations (or ion signals) of the measured organic acids with ambient temperature. The red symbols are data collected from 3 to 27 Sept, while the blue symbols are data collected from 28 Sept onwards. All the data are displayed as 1-hour averages. Black lines shown are linear fits to the datasets.

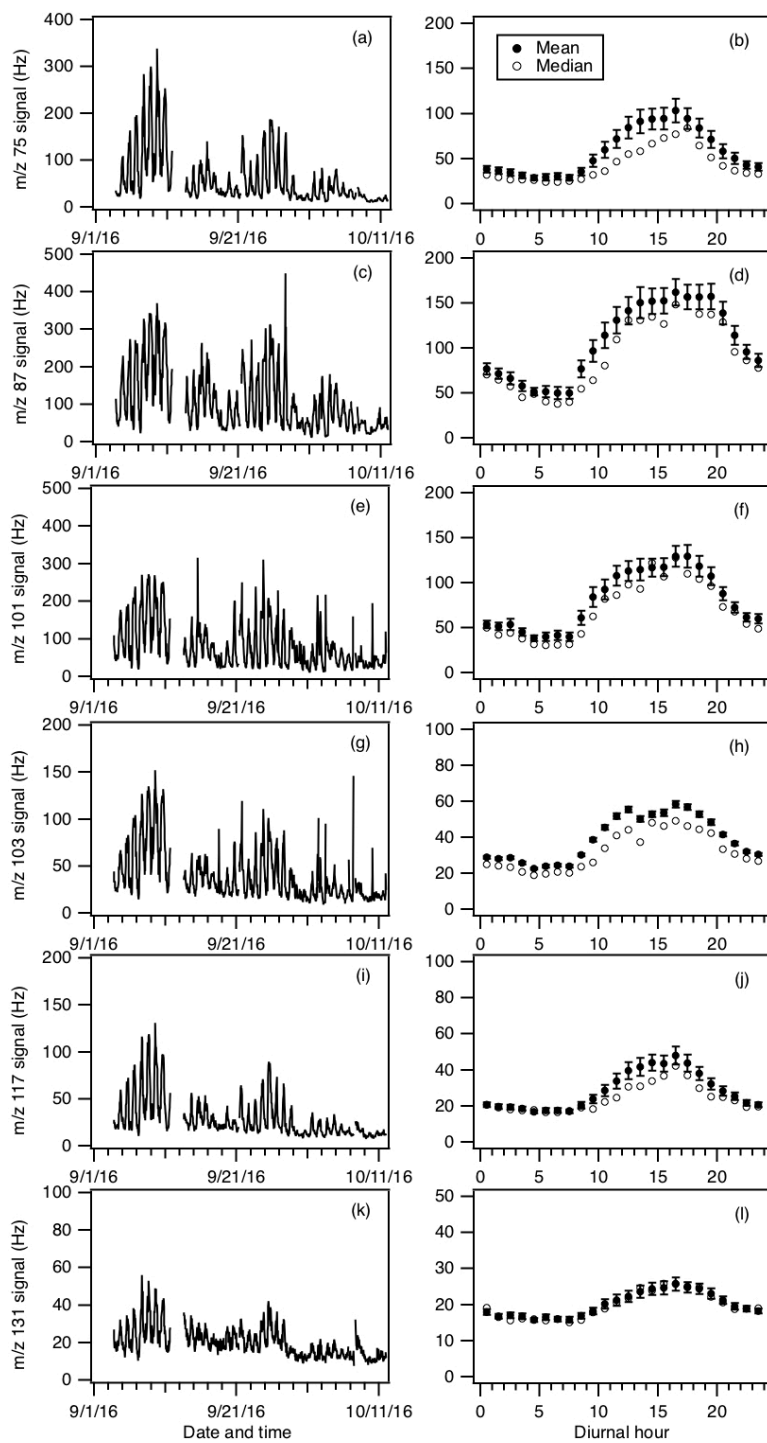


Figure S5: Time series and diurnal profiles of ion signals of organic acids with m/z 75, 87, 101, 103, 117 and 131 measured during the field study. The data are displayed as 1-hour averages. All the signals represent averages in 1-hour intervals and the standard errors are plotted as error bars.

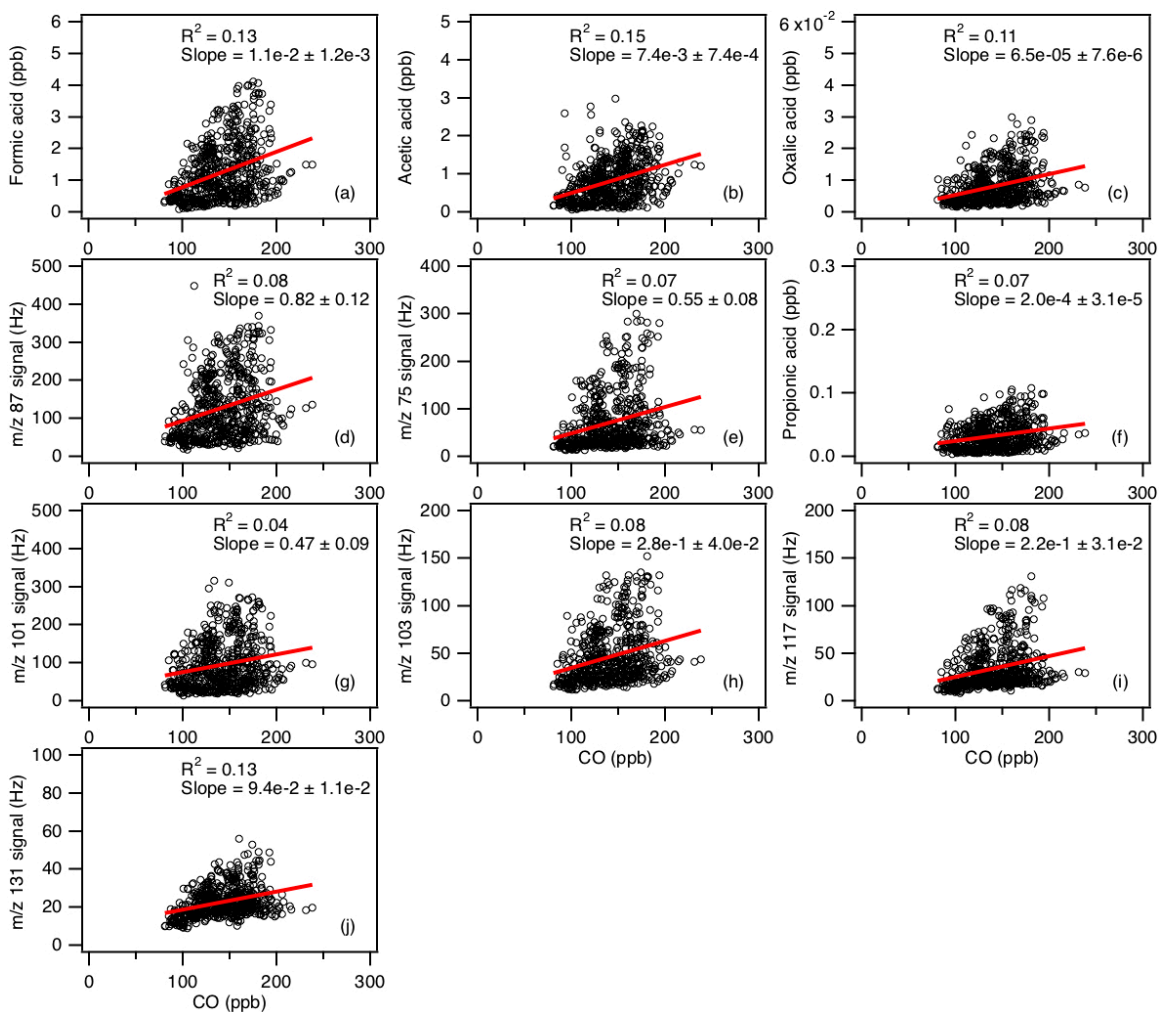


Figure S7: Scatter plots of concentrations (or ion signals) of the measured organic acids with CO concentration. All the data are displayed as 1-hour averages. Red lines shown are linear fits to the data.

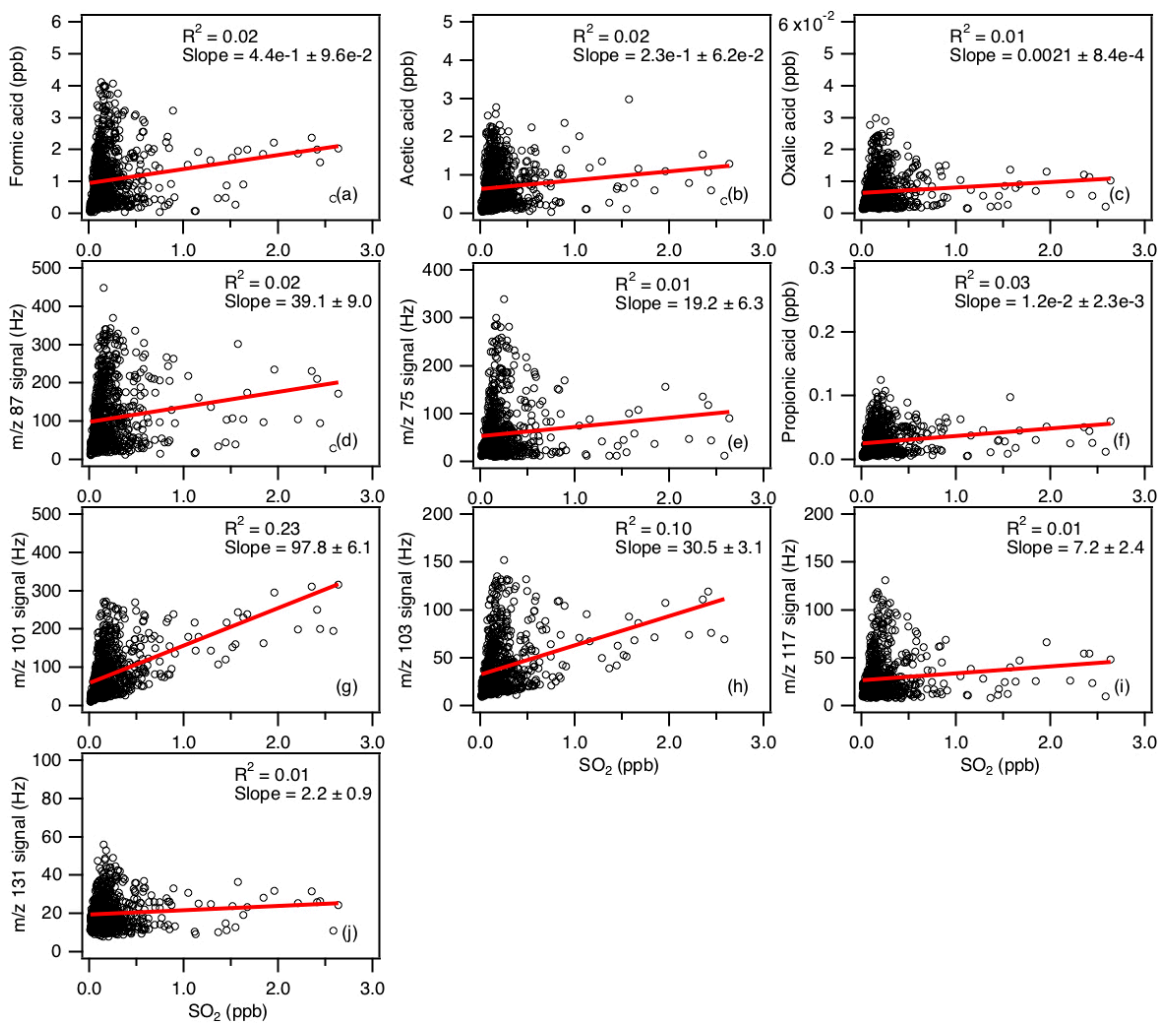


Figure S8: Scatter plots of concentrations (or ion signals) of the measured organic acids with SO₂ concentration. All the data are displayed as 1-hour averages. Red lines shown are linear fits to the data.

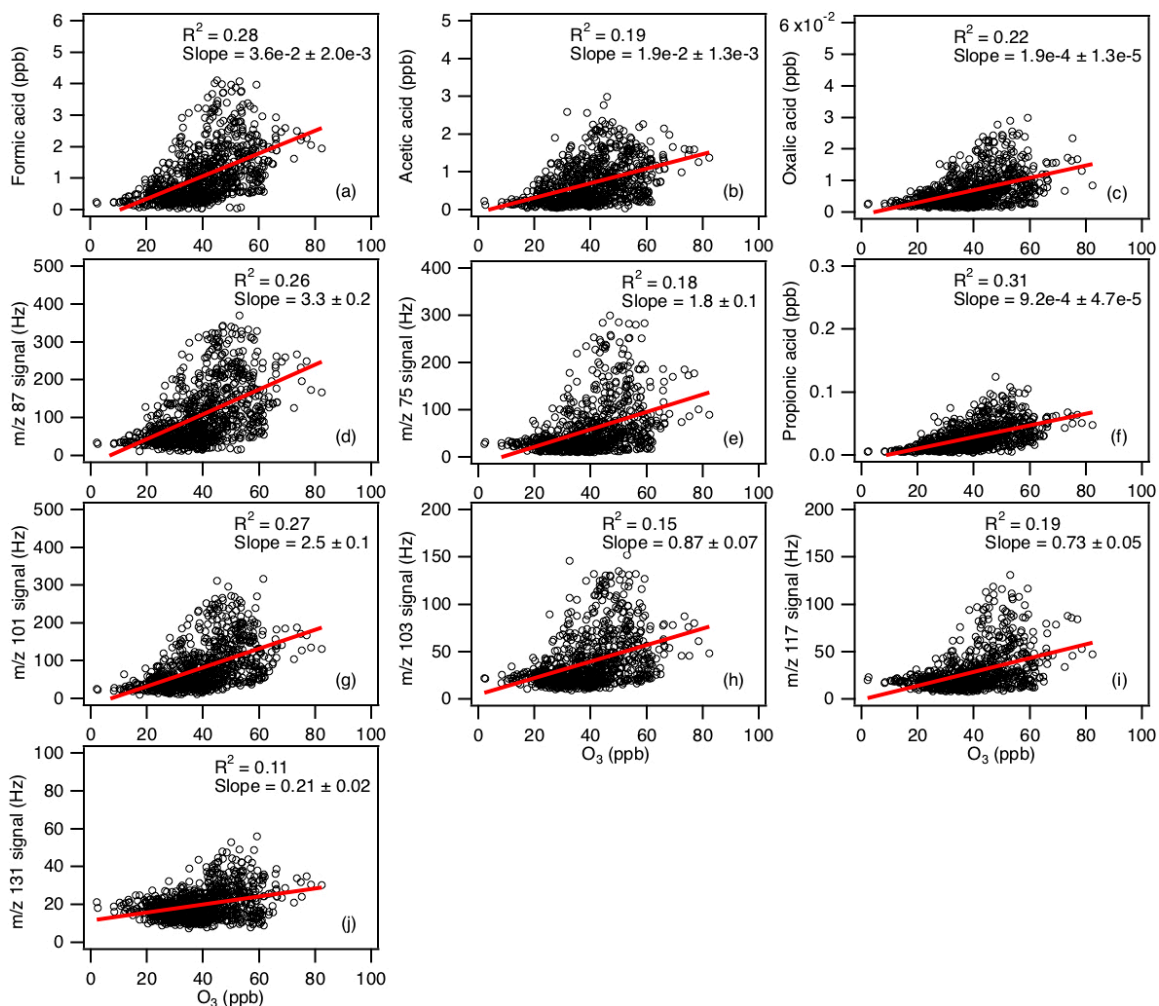


Figure S9: Scatter plots of concentrations (or ion signals) of the measured organic acids with O_3 concentration. All the data are displayed as 1-hour averages. Red lines shown are linear fits to the data.

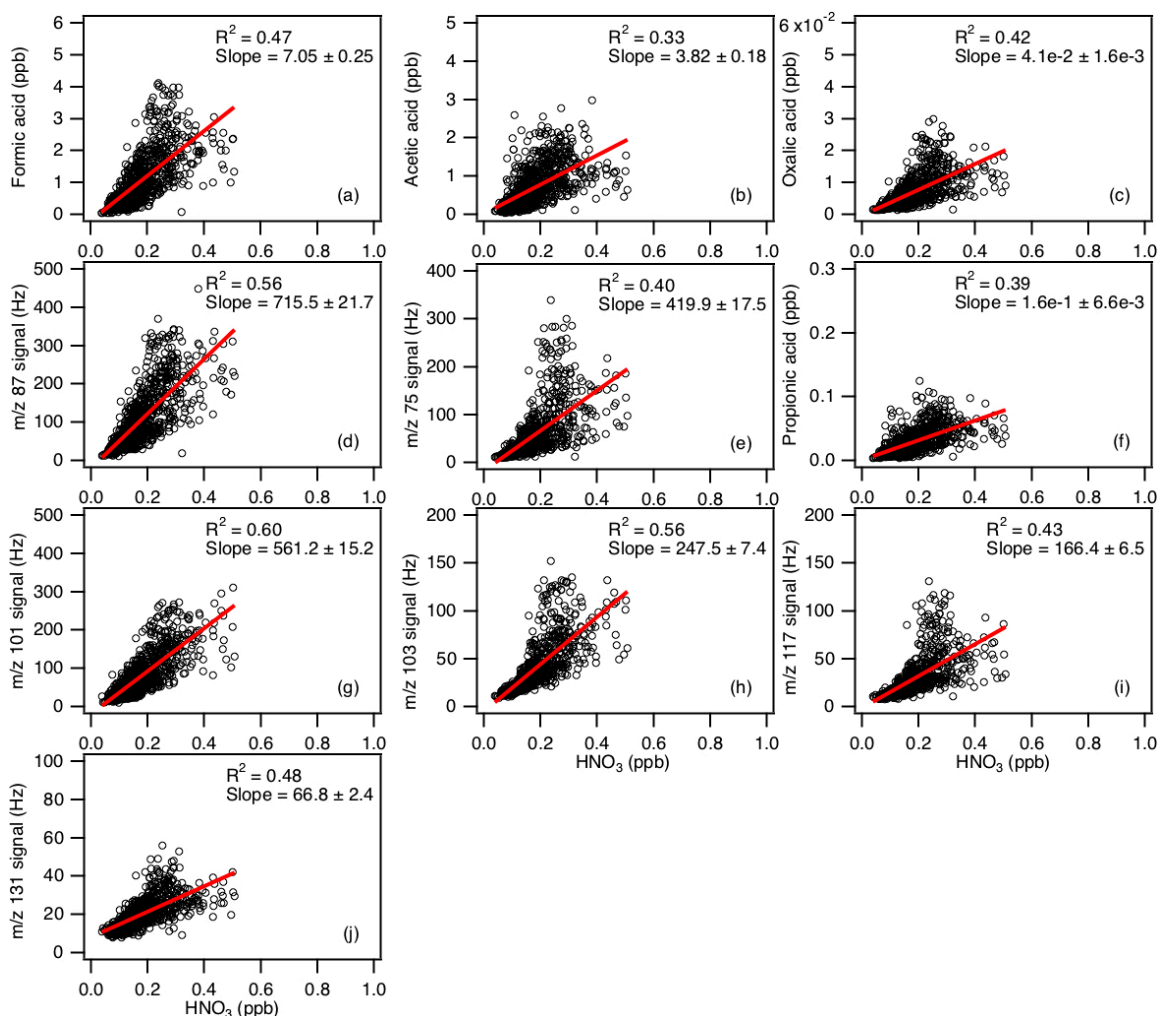


Figure S10: Scatter plots of concentrations (or ion signals) of the measured organic acids with HNO_3 concentration. To exclude periods when the site was affected by urban or power plant emissions, data where $\text{HNO}_3 > 0.5$ ppb are excluded from these scatter plots. All the data are displayed as 1-hour averages. Red lines shown are linear fits to the data.

2. Referee's comment: "Comparison to aerosol composition (section 3.2.3) is not a compelling reason to choose the peak assignments. As is stated in the manuscript, the low volatility compounds measured in the particle phase are expected to have low gas phase concentrations. This could be used to argue that oxalic, malonic... that are present in the particle phase do not explain the signals measured in the CIMS. The IC aerosol measurements are never discussed quantitatively: Do the gas phase concentrations estimated here make sense relative to the particle concentrations?"

Author response: As the IC aerosol measurements have been discussed in detail in another paper, they were not discussed quantitatively in this paper. We refer the referee to Nah et al. (2018) for detailed discussions of the IC aerosol measurements.

Although volatility is a factor, the gas-particle ratios of the organic acids is more complex than that. It depends on thermodynamic conditions, which are dependent on the acid's physicochemical properties (including volatility), ambient temperature, particle water and pH. As explained in detail

in Nah et al. (2018), the measured oxalic acid gas-particle partitioning ratios are in good agreement with their corresponding thermodynamic predictions. Hence, we are confident in our assignment of the m/z 89 ion to oxalic acid since its gas-phase concentrations estimated here make sense relative to its particle concentration. In the case of formic and acetic acids, their measured gas-particle partitioning ratios do not agree with their corresponding thermodynamic predictions, which may be due to mixing states or specific chemical forms of particle-phase formate and acetate (Nah et al., 2018).

Since thermodynamic modeling was not performed for the other organic acids, we are unable to determine if their estimated gas-phase concentrations make sense relative to their particle-phase concentrations. We refer the referee to our reply to comment 1 for revisions made to manuscript regarding the assignment of ions peaks to organic acids.

References:

Nah, T., Guo, H., Sullivan, A. P., Chen, Y., Tanner, D. J., Nenes, A., Russell, A., Ng, N. L., Huey, L. G., and Weber, R. J.: Characterization of Aerosol Composition, Aerosol Acidity and Organic Acid Partitioning at an Agriculture-intensive Rural Southeastern U.S. Site, *Atmos. Chem. Phys. Discuss.*, in review, 10.5194/acp-2018-373, 2018.

3. Referee's comment: *"It would be much more useful to further justify the technique, which may have some advantages over iodide ion chemistry. For example, the sensitivity to propionic acid is much better than iodide. Is the same true for other acids that iodide does not detect well, like acrylic acid? Iodide often suffers from a large lactic acid interference that compromises oxalic acid quantification. What is the sensitivity to lactic acid? Since the motivation was to quantify organic acids, further discussion of the advantages (possibly unique) of SF₆⁻ for quantifying organic acids would be particularly valuable."*

Author response: Since the main purpose of this paper is to introduce SF₆⁻-CIMS as an alternative and promising approach in the detection of organic acids in ambient measurements, the manuscript focuses on the details of the SF₆⁻ ion chemistry and optimal instrument operation for the detection of such acids. Because this paper is not a comparison paper for the different CIMS techniques on the detection of organic acids, we did not conduct laboratory experiments to compare the SF₆⁻ vs. I⁻ sensitivities of different organic acids.

Our preliminary lab experiments showed that SF₆⁻ is less sensitive to lactic acid compared to oxalic acid because the SF₆⁻ + lactic acid reaction results primarily in the formation of SF₅⁻ ions, instead of X⁻ and X•HF ions. As already discussed in the manuscript, the production of SF₅⁻ does not allow for the selective detection of any atmospheric species. In addition, the larger the branching ratio of the SF₅⁻ channel, the lower the CIMS sensitivity to an individual acid since the effective rate constants for the X⁻ and X•HF channels are lower. In addition, we always used gloves when working on the CIMS during this study to limit contamination from emissions from human skin. We also kept people away from the front of the SF₆⁻-CIMS sampling inlet to minimize lactic acid interferences. Furthermore, as noted above, we believe that our assignment of the m/z 89 ion to oxalic acid is reasonable because our estimated gas-phase oxalic acid concentrations make sense relative to its particle concentration. As discussed in detail in Nah et al. (2018), the gas-particle ratios of the organic acids depend of their thermodynamic conditions, which are dependent on the acid's physicochemical properties, ambient temperature, particle water and pH. The measured

oxalic acid gas-particle partitioning ratios were shown to be in good agreement with their corresponding thermodynamic predictions. We refer the referee to our reply to comment 1 for revisions made to manuscript regarding the assignment of m/z 89 to oxalic acid.

Given that the main purpose of this paper is to introduce SF₆⁻-CIMS as an alternative and promising approach in the detection of organic acids in ambient measurements, we feel that we have sufficiently shown the unique advantages of SF₆⁻-CIMS over other reagent ions. As already stated in the manuscript in the introduction, the major advantage that SF₆⁻ has over I⁻ and CH₃CO₂⁻ is that it allows for the detection of acetic acid and SO₂. CF₃O⁻ has a similar chemistry to SF₆⁻ and can detect organic acids but it also has issues due to hydrolysis and the ion precursor is not commercially available. Together, our measurements show that SF₆⁻-CIMS is a promising technique for the simultaneous detection of inorganic species (e.g., SO₂, HNO₃) and organic acids up to C₅ (valeric acid).

References:

Nah, T., Guo, H., Sullivan, A. P., Chen, Y., Tanner, D. J., Nenes, A., Russell, A., Ng, N. L., Huey, L. G., and Weber, R. J.: Characterization of Aerosol Composition, Aerosol Acidity and Organic Acid Partitioning at an Agriculture-intensive Rural Southeastern U.S. Site, *Atmos. Chem. Phys. Discuss.*, in review, 10.5194/acp-2018-373, 2018.

Information regarding how we limited lactic acid contamination during the study has been added to the revised manuscript:

Page 6 line 184: “It should also be noted that we always used gloves when working on the CIMS during this study to limit contamination of lactic acid emissions from human skin. In addition, we kept people away from the front of the SF₆⁻-CIMS sampling inlet to minimize lactic acid interferences as well.”

We have added the following sentences to the revised manuscript to emphasize the high sensitivity of SF₆⁻-CIMS to oxalic, propionic and glycolic acids which are expected to be present at low concentrations in the atmosphere:

Page 23 line 772: “It should be noted that the SF₆⁻ CIMS method is particularly sensitive to oxalic, propionic and glycolic acids, which are expected to be present at low concentrations in the atmosphere.”

4. Referee’s comment: *“I don't understand the normalization to F₂SO₂. F₂SO₂ has a water dependence that the organic acids do not, so the normalization is not appropriate, even if the water dependence is later adjusted (which I didn't understand). Why not normalize to the reagent ion signal, as is common in most other CIMS papers? This would make the work more easily compared to other CIMS techniques, and avoid correcting and then uncorrecting the signals by using F₂SO₂ normalization.”*

Author response: We understand the referee’s point regarding the normalization of signals to F₂SO₂. While it is true that some research groups do normalize their measured signals to the reagent ion signal, this was not carried out in this paper because the SF₆⁻ reagent ion signals were in a region of non-linearity (i.e., at or close to signal saturation) for the entire field study. While we could have corrected for the non-linearity in the SF₆⁻ reagent ion signal prior to normalization,

doing so introduces uncertainties to our measurements. As a point of reference, we can only count linearly to a few hundred thousand ions per second and our counter/detector saturates at about a million ions per second. These numbers are not precise and depend on the particular combination of preamplifier and detector. So, we avoid normalization but instead calibrate often or even continuously.

Although we could have normalized our measured CIMS signals to the sensitivities of the formic or acetic acid calibrant gases, the formic and acetic acid sensitivities were not measured for the entire study because their perm tubes were shared with another CIMS during the study. In contrast, $^{34}\text{SO}_2$ was the main calibrant gas and its sensitivity was measured during every calibration period for the entire field study. Consequently, the CIMS instrument sensitivity measured by the $\text{F}_2^{34}\text{SO}_2^-$ ion signal was applied to all the measured species (except for formic and acetic acids during periods when their perm tubes were used for calibration purposes by the SF_6^- -CIMS) using relative sensitivities determined in laboratory studies.

5. Referee's comment: "*With the removal of speculation in sections 3.24 and 3.3, there is room to emphasize some of the measurement technique accomplishments. The reagent ion signal is never mentioned in the text, though it is stated in the authors comments. Achieving a signal of 9 MHz is extraordinary given the low activity of the ionizer. Few CIMS do any better than this, so lines 352-354 are not correct in general. The paper should detail how the large reagent ion signal was achieved, as this seems to be a major new advance.*"

Author response: We disagree that the SF_6^- reagent ion signal is extraordinarily high and that lines 352 to 354 are incorrect. It may be true that some commercial CIMS can't achieve such high levels of reagent ion signal, but our group has achieved this level of SF_6^- and I^- reagent ion signals ($>10^6$ Hz) with our custom-built CIMS for many years. We refer the referee to Fig. 5 of Slusher et al. (2004) for an example of the I^- reagent ion signal ($\sim 10^6$ Hz) obtained during a previous field study in 2002. In this example, the I^- signal was also saturated at an apparent signal of 10^6 Hz and was probably more on the order of 10 MHz if it could be counted accurately.

The obtainment of such high levels of reagent ion signals by our CIMS is probably due to the evolution of the design of our CIMS. This has been documented extensively, and we refer the referee to Liao et al. (2011) (or other previous papers from our group) for a more detailed description of our instrument.

References:

Liao, J., Sihler, H., Huey, L. G., Neuman, J. A., Tanner, D. J., Friess, U., Platt, U., Flocke, F. M., Orlando, J. J., Shepson, P. B., Beine, H. J., Weinheimer, A. J., Sjostedt, S. J., Nowak, J. B., Knapp, D. J., Staebler, R. M., Zheng, W., Sander, R., Hall, S. R., and Ullmann, K.: A comparison of Arctic BrO measurements by chemical ionization mass spectrometry and long path-differential optical absorption spectroscopy, *Journal of Geophysical Research-Atmospheres*, 116, 10.1029/2010jd014788, 2011.

Slusher, D. L., Huey, L. G., Tanner, D. J., Flocke, F. M., and Roberts, J. M.: A thermal dissociation-chemical ionization mass spectrometry (TD-CIMS) technique for the simultaneous measurement of peroxyacyl nitrates and dinitrogen pentoxide, *Journal of Geophysical Research-Atmospheres*, 109, 13, 10.1029/2004jd004670, 2004.

6. Referee's comment: "*Likewise, the high sensitivity to acetic acid and possible insensitivity to lactic acid are important. The former is discussed, but it would be more powerful to have a table that compares the sensitivities here for all the acids to other CIMS techniques.*"

Author response: We disagree with the referee's assertion on the need for a table that compares the SF₆⁻ sensitivities of all the organic acids to other reagent ions. The main purpose of this paper is to introduce SF₆⁻-CIMS as an alternative and promising approach in the detection of organic acids in ambient measurements. This paper is not a comparison paper for the different CIMS techniques on the detection of organic acids. In addition, we think a table comparing sensitivities is likely to be misleading as instruments are constantly developing and being used in different configurations. Hence, the manuscript focuses on the details of the SF₆⁻ ion chemistry and optimal instrument operation for the detection of such acids.

Given the main purpose of this paper, we strongly feel that we have sufficiently shown the advantages of SF₆⁻-CIMS over other reagent ions such as CH₃CO₂⁻, I⁻ and CF₃O⁻ to justify it being a promising technique in the detection of ambient organic acids. As already stated in the manuscript and in our previous reply to comment 1 from referee 2, the major advantage that SF₆⁻ has over I⁻ and CH₃CO₂⁻ is that it allows for the detection of acetic acid and SO₂. CF₃O⁻ has a similar chemistry to SF₆⁻ and can detect organic acids but it also has issues due to hydrolysis and the ion precursor is not commercially available. Together, our measurements show that SF₆⁻-CIMS is a promising technique for the simultaneous detection of inorganic species (e.g., SO₂, HNO₃) and organic acids up to C₅ (valeric acid).

The referee's comment regarding the SF₆⁻ sensitivity to lactic acid is addressed in our replies to comment 1 and 3.

7. Referee's comment: "*The 1/e2 time decays are given, but the time response for most of the system is very fast. It looks like 1/e is <13s. Where does the time response come from? It is slower than many other CIMS measurements, even though there is a very large flow through the flow tube, and the inlet appears to be only 25 cm and with a large flow. Do the high dilution or reduced pressure affect time response?*"

Author response: Determination of the time response of our CIMS is limited by the CIMS sampling time. As stated in the manuscript, the sampling conditions of the CIMS during the study resulted in 13 s time resolution data. Hence, it is not possible to accurately determine the times for the various signals to decay to 1/e since it appears that the times all appear to be ≤ 13 s. We did not put this in the first version of the paper for these reasons and only did so at the suggestion of a reviewer. In addition, as stated in the manuscript, we report 1-hour averaged ambient concentrations (not 13 s ambient concentrations), which is sufficient for the purpose of this ground-based field study where the concentrations of measured species do not change rapidly (unlike airborne campaigns). Hence, we do not expect the time response of our CIMS to affect our results and conclusions.

However, the high dilution and reduced pressure do not affect the CIMS time response relative to other configurations of our CIMS. Instead, we expect the CIMS time response to a species to be governed primarily by the species' propensity to adhere to surfaces. This information has been added to the revised manuscript:

Page 15 line 450: “The CIMS time response to a compound is governed primarily by the compound’s propensity to adhere to surfaces. The decays in the formic and acetic acid ion signals and times required for them to reach steady state after the removal of calibration gases during the switch from standard addition calibration to ambient sampling were used to determine the CIMS response time.”

8. Referee’s comment: *“line 242: what were the impurities in glyoxylic?”*

Author response: We were unable to identify the impurities in our glyoxylic acid. Although the purity of the sample was listed as 98 % by the manufacturer (Sigma Aldrich), the impurities were not listed. Some of these m/z peaks appeared at masses larger than glyoxylic acid, suggesting that they may be polymers.

9. Referee’s comment: *“line 244: what are the vapor pressures? would heating generate sufficient vapor pressure?”*

Author response: The vapor pressures of malonic, succinic and glutaric acids are 5.73×10^{-4} , 1.13×10^{-4} and 4.21×10^{-4} kPa at 298 K, respectively (Booth et al., 2010). Although the referee is correct in stating that heating the malonic, succinic and glutaric acid samples will likely generate sufficient vapors for calibration, this method of generating calibrant gases for calibration purposes is subjected to errors caused by the vapors condensing out and adhering onto surfaces at room temperature prior to introduction into the CIMS. It is very difficult to maintain all parts of the tubing, inlet, and CIMS at an elevated temperature which would be required if we used a heated sample. This information has been added to the revised manuscript:

Page 9 line 249: “We attempted to generate calibration plots for malonic (Sigma Aldrich, \geq 99.5 %), succinic (Sigma Aldrich, 99 %) and glutaric (Sigma Aldrich, 99 %) acids by passing N_2 over their solid samples at room temperature. However, it was not possible to generate large enough gas phase concentrations for calibration since these organic acids have very low vapor pressures. The vapor pressures of malonic, succinic and glutaric acids are 5.73×10^{-4} , 1.13×10^{-4} and 4.21×10^{-4} kPa at 298 K, respectively (Booth et al., 2010), which are at least 2 orders of magnitude lower than the organic acids that we calibrated for. Although heating up the malonic, succinic and glutaric acid samples will likely generate sufficient vapors for calibration, this method of generating calibrant gases will lead to large measurement uncertainties due to vapors condensing out and adhering onto surfaces at room temperature prior to introduction into the CIMS.”

References:

Booth, A. M., Barley, M. H., Topping, D. O., McFiggans, G., Garforth, A., and Percival, C. J.: Solid state and sub-cooled liquid vapour pressures of substituted dicarboxylic acids using Knudsen Effusion Mass Spectrometry (KEMS) and Differential Scanning Calorimetry, *Atmos. Chem. Phys.*, **10**, 4879-4892, 10.5194/acp-10-4879-2010, 2010.

10. Referee’s comment: *“line 353: how much higher can the sensitivity and Po210 activity go?”*

Author response: A new commercial ^{210}Po ion source typically has 20 mCi activity. We estimate that the sensitivities may increase by as much as a factor of 5 with a new ^{210}Po ion source. This information has been added into the revised manuscript:

Page 12 line 382: “A weak ^{210}Po ion source (< 1 mCi) was used by SF_6 -CIMS instrument during the field study, hence these sensitivities will be substantially higher if a stronger radioactive source is used. Post-field laboratory work suggest that the sensitivities may increase by as much as a factor of 5 for a new commercial 20 mCi ^{210}Po ion source.”

11. Referee’s comment: “line 393: replace “noticeable increase” with “xx% increase”.”

Author response: As requested, this information has been added into the revised manuscript:

Page 14 line 425: “There is a ~50 % increase in the $\text{F}_2^{34}\text{SO}_2^-/^{34}\text{SF}_6^-$ ion signal ratio on 28 Sept 2016, indicating an increase in the CIMS instrument sensitivity.”

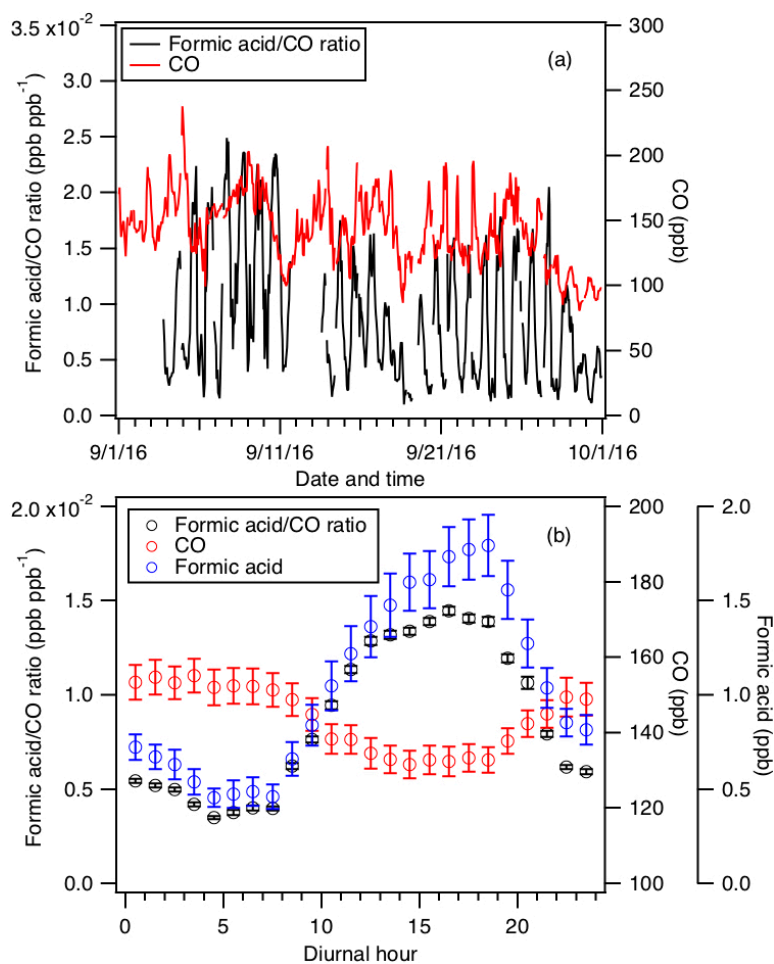
12. Referee’s comment: “line 406: how was water vapor dependence accounted for?”

Author response: The water vapor dependence was accounted for using the linear relationship between the $\text{F}_2^{34}\text{SO}_2^-$ ion sensitivity and ambient water vapor concentration shown in Fig. S2c. This information has been added into the revised manuscript:

Page 14 line 438: “We accounted for water vapor dependence of the $\text{F}_2^{34}\text{SO}_2^-$ ion signal using the linear relationship between the $\text{F}_2^{34}\text{SO}_2^-$ ion sensitivity and ambient water vapor concentration (Fig. S2c) in our post-field calibrations, where the response of the CIMS acid signals were measured relative to the of the $^{34}\text{SO}_2$ sensitivity.”

13. Referee’s comment: “section 3.2.1: ratios to CO may be helpful, in case transported air explains increase.”

Author response: The formic acid/CO ratios ranged from 1.0×10^{-3} to 2.5×10^{-2} ppb ppb $^{-1}$, with an average of $8.7 \times 10^{-3} \pm 5.8 \times 10^{-3}$ ppb ppb $^{-1}$. The CO concentrations were consistently low during the study and ranged from 80 to 240 ppb, with consistent diurnal trends (see Fig. a below). Since the CO concentrations and diurnal profile have been published in another paper (Nah et al. 2018), they were not shown in this manuscript. Based on the diurnal profile of the formic acid/CO ratio (see Fig. b below), the formic acid/CO ratio peaks in the mid-afternoon, which coincides with when formic acid and CO reach their maximum and minimum, respectively.



Given that 1) the CO concentration did not spike during the field study, 2) the formic acid has a consistent diurnal profile, and 3) the formic acid/CO ratio time series is consistent with the diurnal trends of CO and formic acid, it is unlikely that the increase in that the increase in formic acid during the day can be explained by transported CO. This information has been added to the revised manuscript:

Page 21 line 702: “Formic acid/CO ratios (which have been used in some studies to determine the contribution of polluted air masses) ranged between 1.0×10^{-3} to 2.5×10^{-2} ppb ppb⁻¹. The ratio peaked consistently in the mid-afternoon, which coincided with when formic acid and CO reached their maximum and minimum, respectively. In addition, there were no spikes in the formic acid/CO ratio during the study, suggesting that contributions of polluted air masses to the daily increase in formic acid are minimal.”

14. Referee’s comment: “line 535: I don't understand comparison of organic ion signal to F2SO2 sensitivity. the ratio here isn't unitless.”

Author response: We acknowledge that the units used are confusing. Hence, we will use the raw ion signals (Hz) of m/z 75, 87, 101, 103, 117 and 131 in the revised manuscript. The revised figures are shown in our reply to comment 1.

15. Referee’s comment: “line 559: what does zeroth order check mean?”

Author response: It means that we checked that the estimated sum of organic carbon contributed by the measured organic acids is consistent with the total gas-phase water-soluble organic carbon (WSOC_g). Since the estimated carbon mass fractions of WSOC_g comprised of these organic acids are generally less than 100 %, this suggests that our peak assignments are plausible. To remove any confusion, we have modified the aforementioned sentence in the revised manuscript:

Page 19 line 602: “This comparison primarily serves as a check to determine if the peak assignments are plausible by ensuring that the estimated sum of organic carbon contributed by these four organic acids is less than or equal to the measured WSOC_g.”

16. Referee’s comment: *“line 591: How long are these spikes? How close is the nearest power plant or urban area?”*

Author response: The SO₂ and HNO₃ spikes can last between 1 to 3 hours. The closest power plant was Plant Bowen, which was ~25 km north of the site. The closest urban center was Atlanta, which was ~55 km away. This information has been added to the revised manuscript:

Page 5 line 125: “Briefly, the Yorkville field site (33.931 N, 85.046 W) was located ~55 km northwest of Atlanta (the closest urban center), and was on a broad ridge in a large pasture where there were occasionally grazing cattle. The field site was surrounded by forest and agricultural land. There were no major roads near the field site and nearby traffic emissions were negligible. The closest power plant was Plant Bowen, which was located ~25 km north of the field site.”

Page 20 line 669: “However, there were occasional periods when the site was impacted by anthropogenic pollution. In particular, there are spikes in both SO₂ and HNO₃ concentrations lasting between 1 to 3 hours throughout the study that corresponded to the site being impacted by power plant or urban emissions.”

17. Referee’s comment: *“line 663: what is a reasonable detection limit? give a number”*

Author response: Whether or not a detection limit is reasonable will depend on the species measured. In this study, our detection limits for the organic acids studied (1 to 60 ppt) are typically lower than the concentrations of the organic acids studied, allowing us to be reasonably confident of the concentrations measured. To remove any confusion, we have modified the aforementioned sentence in the revised manuscript:

Page 23 line 771: “Limits of detection ranged from 1 to 60 ppt for 2.5 min integration periods for the organic acids studied.”

18. Referee’s comment: *“Please define all acronyms at first use. I could not find definitions for m/z, slpm.”*

Author response: These definitions have been added to the revised manuscript.

1 **Real-time measurements of gas-phase organic acids using SF₆⁻ chemical ionization**
2 **mass spectrometry**

3
4 Theodora Nah,^{1,a} Yi Ji,^{1,2} David J. Tanner,¹ Hongyu Guo,¹ Amy P. Sullivan,³ Nga Lee
5 Ng,^{1,2} Rodney J. Weber¹ and L. Gregory Huey^{1*}

6
7 ¹*School of Earth and Atmospheric Sciences, Georgia Institute of Technology, Atlanta, GA, USA*

8 ²*School of Chemical and Biomolecular Engineering, Georgia Institute of Technology, Atlanta, GA, USA*

9 ³*Department of Atmospheric Science, Colorado State University, Fort Collins, CO, USA*

10 ^a*Now at School of Energy and Environment, City University of Hong Kong, Kowloon, Hong Kong, China*

11 * *To whom correspondence should be addressed: greg.huey@eas.gatech.edu*

Formatted: Font: 10 pt, Italic, Superscript

Formatted: Line spacing: single

Formatted: Font: 10 pt, Italic

13 **Abstract**

14 The sources and atmospheric chemistry of gas-phase organic acids are currently poorly
15 understood due in part to the limited range of measurement techniques available. In this
16 work, we evaluated the use of SF₆⁻ as a sensitive and selective chemical ionization reagent
17 ion for real-time measurements of gas-phase organic acids. Field measurements are made
18 using a chemical ionization mass spectrometer (CIMS) at a rural site in Yorkville, Georgia
19 from September to October 2016 to investigate the capability of this measurement
20 technique. Our measurements demonstrate that SF₆⁻ can be used to measure a range of
21 organic acids in the atmosphere. 1-hour averaged ambient concentrations of organic acids
22 ranged from a few parts per trillion by volume (ppt) to several parts per billion by volume
23 (ppb). All the organic acids displayed similar strong diurnal behaviors, reaching maximum
24 concentrations between 5 and 7 pm local time. The organic acid concentrations are
25 dependent on ambient temperature, with higher organic acid concentrations being
26 measured during warmer periods.

27 **Introduction**

28 Organic acids are ubiquitous and important species in the troposphere. They are
29 major contributors of free acidity in precipitation (Galloway et al., 1982; Keene et al., 1983;
30 Keene and Galloway, 1984), and can also affect the formation of secondary organic
31 aerosols (SOA) (Zhang et al., 2004; Carlton et al., 2006; Sorooshian et al., 2010; Yatavelli
32 et al., 2015). As end products of oxidation, organic acids can also serve as useful tracers of
33 air mass history (Sorooshian et al., 2007; Sorooshian et al., 2010). Organic acids are found
34 in urban, rural and remote marine environments in the gas, aqueous and particle phases.

35 While organic acids are emitted directly from biogenic sources (e.g., microbial activity,
36 vegetation and soil) and anthropogenic activities (e.g., fossil fuel combustion, vehicular
37 emissions and biomass burning) (Kawamura et al., 1985; Talbot et al., 1988; Chebbi and
38 Carlier, 1996; Talbot et al., 1999; Seco et al., 2007; Veres et al., 2010; Paulot et al., 2011;
39 Veres et al., 2011; Millet et al., 2015), they can also be formed from photooxidation of
40 non-methane volatile organic compounds and aqueous-phase photochemistry of semi-
41 volatile organic compounds (Chebbi and Carlier, 1996; Hansen et al., 2003; Orzechowska
42 and Paulson, 2005; Carlton et al., 2006; Sorooshian et al., 2007; Ervens et al., 2008; Paulot
43 et al., 2011; Millet et al., 2015). The chemical aging of organic aerosols has also been
44 proposed as a major source of organic acids (Molina et al., 2004; Vlasenko et al., 2008;
45 Paulot et al., 2011). The relative importance of primary and secondary sources of organic
46 acids are currently poorly constrained though their emissions likely depend on the
47 magnitude of biogenic and anthropogenic activities and the meteorological conditions. Wet
48 and dry deposition are the primary sinks of organic acids in the atmosphere (Chebbi and
49 Carlier, 1996).

50 Formic and acetic acids are the dominant gas-phase monocarboxylic acids in the
51 troposphere (Chebbi and Carlier, 1996). Due to their high vapor pressures, the gas-phase
52 concentrations of formic and acetic acids are usually 1 to 2 orders of magnitudes higher
53 than their particle-phase concentrations. Some field studies report strong correlations
54 between formic and acetic acids, suggesting that these two organic acids have similar
55 sources (Nolte et al., 1997; Souza and Carvalho, 2001; Paulot et al., 2011). A recent
56 modeling study suggested that the dominant sources of formic acid in the southeastern U.S.
57 are primarily biogenic in nature (Millet et al., 2015). These sources include direct emissions
58 from vegetation and soil and photochemical production from biogenic volatile organic
59 compounds (BVOCs). Currently, atmospheric formic and acetic acid concentrations are
60 higher than those predicted by models, indicating that present model estimates of source
61 and sink magnitudes are incorrect (Paulot et al., 2011; Millet et al., 2015). In the case of
62 formic acid, deposition and secondary photochemical production via mechanisms such as
63 photooxidation of isoprene and reaction of stabilized criegee intermediates need to be
64 better constrained in models. Given that formic and acetic acids are major trace gases in
65 the atmosphere, there is a need to resolve the discrepancy between measurements and

66 model predictions to close the atmospheric reactive carbon budget and improve our overall
67 understanding of VOC chemistry in the atmosphere.

68 Currently, research on gas-phase organic acids has focused primarily on formic and
69 acetic acids (Andreae et al., 1988; Talbot et al., 1988; Grosjean, 1991; Hartmann et al.,
70 1991; Talbot et al., 1995; Talbot et al., 1999). This is due, in part, to the analytical
71 difficulties in measuring gas-phase $> C_2$ organic acids and oxidized organic acids (i.e.,
72 containing more than 2 oxygen atoms) in real time. These organic acids have low vapor
73 pressures and are generally present in low concentrations in the gas phase. For example,
74 dicarboxylic acids typically have vapor pressures that are 2 to 4 orders of magnitude lower
75 than their analogous monocarboxylic acids (Chebbi and Carlier, 1996), and are present
76 mainly in the particle and aqueous phases. Rapid and accurate measurements of gas-phase
77 $> C_2$ organic acids and oxidized organic acids are necessary for constraining the regional
78 and global SOA budget since these acids can partition readily between the gas and particle
79 and aqueous phases and subsequently affect SOA formation (Zhang et al., 2004; Carlton
80 et al., 2006; Ervens et al., 2008; Sorooshian et al., 2010; Yatavelli et al., 2015).

81 Chemical ionization mass spectrometry (CIMS) is commonly used to selectively
82 measure atmospheric trace gases in real-time with high sensitivity. CIMS measurements
83 rely on reactions between reagent ions and compounds of interest present in the sampled
84 air to produce analyte ions that are detected by a mass spectrometer. The subset of
85 molecular species detected is determined by the reagent ion employed since the specificity
86 of the ionization process is governed by the ion-molecule reaction mechanism. CIMS is a
87 popular tool for atmospheric measurements since it is versatile and has high time resolution
88 and sensitivity. It is also often a soft ionization technique with minimal ion fragmentation,
89 thus preserving the parent molecule's elemental composition and allowing for molecular
90 speciation. Recent developments in chemical ionization methods and sources have greatly
91 improved our ability to measure atmospheric acidic species. Some of the CIMS reagent
92 ions that have been used to measure atmospheric organic acids include acetate ($CH_3CO_2^-$),
93 iodide (I^-) and CF_3O^- anions (Crounse et al., 2006; Veres et al., 2008; Lee et al., 2014;
94 Brophy and Farmer, 2015; Nguyen et al., 2015). However, each of these CIMS reagent
95 ions has its drawbacks, which are generally related to their selectivity and sensitivity

96 towards different atmospheric species. For example, acetic acid is difficult to measure with
97 CH_3CO_2^- as the CIMS reagent ion due to interferences from the reagent ion chemistry that
98 complicates the desired ion-molecule reactions. In addition, while many organic acids can
99 be detected using I^- as a reagent ion, its sensitivity to different acids can vary by orders of
100 magnitude (Lee et al., 2014).

101 The sulfur hexafluoride (SF_6^-) anion has been used as a CIMS reagent ion to
102 measure atmospheric inorganic species such as sulfur dioxide (SO_2), nitric acid (HNO_3)
103 and peroxyxynitric acid (HO_2NO_2) (Slusher et al., 2001; Slusher et al., 2002; Huey et al.,
104 2004; Kim et al., 2007). SF_6^- commonly reacts with most acidic gases at the collision rate
105 by either proton or fluoride transfer reactions (Huey et al., 1995). The SF_6^- ion chemistry
106 is selective to acidic species, which can simplify the mass spectral analysis of organic acids.
107 However, SF_6^- is reactive to both ozone (O_3) and water vapor, which can lead to interfering
108 reactions that limit its applicability to many species in certain environments (Huey et al.,
109 2004). For these reasons, this work is focused on assessing the ability of SF_6^- to measure a
110 series of organic acids in ambient air. The major advantage that SF_6^- has over I^- and
111 CH_3CO_2^- is that it allows for the detection of acetic acid and SO_2 . CF_3O^- has a similar
112 chemistry to SF_6^- but it also has issues due to hydrolysis and the ion precursor is not
113 commercially available. We present ambient measurements of gas-phase organic acids
114 conducted in a mixed forest-agricultural area in Georgia in early fall of 2016 to evaluate
115 the performance of a SF_6^- CIMS technique. Gas-phase organic acid measurements are
116 compared to gas-phase water-soluble organic carbon (WSOC_g) measurements performed
117 during the field study to estimate the fraction of WSOC_g that is comprised of organic acids
118 at this rural site. Laboratory experiments are conducted to measure the sensitivity of SF_6^-
119 with a series of organic acids of atmospheric relevance.

120 **2. Methods**

121 **2.1. Field site**

122 Real-time ambient measurements of gas-phase organic acids were obtained using a
123 chemical ionization mass spectrometer from 3 Sept to 12 Oct 2016 at the SouthEastern
124 Aerosol Research and Characterization (SEARCH) site located in Yorkville, Georgia. A

125 detailed description of the field site has been provided by Hansen et al. (2003). Briefly, the
126 Yorkville field site (33.931 N, 85.046 W) was located ~55 km northwest of Atlanta (the
127 closest urban center), and was on a broad ridge in a large pasture where there were
128 occasionally grazing cattle. The field site was surrounded by forest and agricultural land.
129 There were no major roads near the field site and nearby traffic emissions were negligible.
130 The closest power plant was Plant Bowen, which was located ~25 km north of the field
131 site. The sampling period was characterized by moderate temperatures (24.0 °C average,
132 32.6 °C max, 9.5 °C min) and high relative humidities (68.9 % RH average, 100 % RH
133 max, 21.6 % RH min). The study-averaged diurnal trends of relative humidity, temperature
134 and solar radiance are shown in Fig. S1. Data reported are displayed in EDT. Volumetric
135 gas concentrations reported are at ambient temperature and relative humidity.

136 2.2. SF₆ CIMS

137 2.2.1. CIMS instrument and air sampling inlet

138 The CIMS instrument was housed in a temperature-controlled trailer during the
139 field study. The inlet configuration and CIMS instrument used in this study is shown in
140 Fig. 1. Since HNO₃ and organic acids may condense on surfaces, an inlet configuration
141 with a minimal wall interaction was used. This inlet configuration was previously described
142 by Huey et al. (2004) and Nowak et al. (2006); hence, only a brief description will be
143 provided here. The inlet was a 7.6 cm ID aluminum pipe that extended ~40 cm into the
144 ambient air through a hole in the trailer's wall. This positioned the inlet ~2 m above the
145 ground. A donut-shaped ring was attached to the ambient sampling port of the pipe to
146 reduce the influence of crosswinds on the pipe's flow dynamics. This ring was wrapped
147 with a fine wire mesh to prevent insects from being drawn through the pipe. A flow of
148 ~2800 L min⁻¹ was maintained in the pipe using a regenerative blower (AMETEK
149 Windjammer 116637-03). Part of this flow (7 L min⁻¹) was sampled through a custom-
150 made three-way PFA Teflon valve, which connected the pipe's center to the CIMS
151 sampling orifice. The valve was maintained at a temperature of 40 °C in an insulated
152 aluminum oven and could be switched automatically between ambient and background
153 modes. In ambient mode, ambient air was passed through a 25 cm long, 0.65 cm ID Teflon

Deleted: temperature controlled

155 tube into the CIMS. In background mode, ambient air was first drawn through an activated
156 charcoal scrubber before being delivered into the CIMS. A small flow of ambient air (~ 0.05
157 L min^{-1}) was continuously passed through the scrubber to keep it at equilibrium with
158 ambient humidity levels. Most of the sampled air flow (6.7 L min^{-1}) was exhausted using
159 a small diaphragm pump. The rest of the sampled air flow (0.3 L min^{-1}) was introduced
160 into the CIMS instrument through an automatic variable orifice, which was used to
161 maintain a constant sample air mass flow.

162 The CIMS instrument was comprised of a series of differentially pumped regions:
163 a flow tube, a collisional dissociation chamber, an octopole ion guide, a quadrupole mass
164 filter and an ion detector. These sections were evacuated by a scroll pump (Edward nXDS
165 20i), a drag pump (Adixen MDP 5011) and two turbo pumps (Varian Turbo-V301),
166 respectively. Ambient air was drawn continuously into the flow tube. A flow of 3.7
167 standard liter per minute (slpm) of N_2 containing a few ppm of SF_6 (Scott-Marrin Inc.) was
168 passed through a ^{210}Po ion source into the flow tube. SF_6^- anions, which were produced via
169 associative electron attachment in the ^{210}Po ion source, reacted with the sampled ambient
170 air in the flow tube to generate analyte ions. Arnold and Viggiano (2001) showed that the
171 formation of $\text{F}\cdot(\text{HF})_n$ cluster ions from the reaction of SF_6^- and water vapor is enhanced at
172 high flow tube pressures. Since these $\text{F}\cdot(\text{HF})_n$ cluster ions could interfere with mass
173 spectral analysis, the flow tube was maintained at a low pressure ($\sim 13 \text{ mbar}$, 0.5 %
174 uncertainty) in this study to reduce both the water vapor concentration and reaction time in
175 the flow tube, thus minimizing interferences from SF_6^- reaction with water vapor. The
176 analyte ions exited the flow tube and were accelerated through the collisional dissociation
177 chamber (CDC), which was maintained at $\sim 0.8 \text{ mbar}$ (10 % uncertainty). The molecular
178 collisions in the CDC served to dissociate weakly bound cluster ions into their core ions to
179 simplify mass spectral analysis. Flow tube and CDC pressures were controlled by the
180 automatic variable orifice. For this study, the CDC was operated at a relatively high electric
181 field ($\sim 113 \text{ V cm}^{-1}$) to efficiently dissociate cluster ions. The resulting ions were then
182 passed into the octopole ion guide (maintained at $\sim 6 \times 10^{-3} \text{ mbar}$), which collimated the
183 ions and transferred them into the quadrupole mass spectrometer (maintained at $\sim 10^{-5}$
184 mbar) for mass selection and detection. It should also be noted that we always used gloves
185 when working on the CIMS during this study to limit contamination of lactic acid

186 emissions from human skin. In addition, we kept people away from the front of the SF₆-
187 CIMS sampling inlet to minimize lactic acid interferences as well.

188 Ions monitored during the field study included mass-to-charge ratio (m/z) 45, 59,
189 65, 73, 75, 79, 82, 87, 89, 101, 102, 103, 108, 117, 131 and 148. The assignment of these
190 ions will be discussed in section 3. The dwell time for each m/z ion was set to 0.5 s and
191 measurements of these ions were obtained every ~13 s, which resulted in a ~4 % (= 0.5/13
192 x 100 %) duty cycle for each ion monitored. The data presented in this paper was averaged
193 to 1-hour intervals unless stated otherwise.

194 **2.2.2. Background and calibration measurements during field study**

195 Background measurements were performed every 25 min during the field study.
196 During each background measurement, the sampled air flow was passed through an
197 activated charcoal scrubber prior to delivery into the CIMS. The scrubber removed > 99 %
198 of the targeted species in ambient air. Calibration measurements were performed every 5 h
199 during the field study through standard additions of ³⁴SO₂ and either formic or acetic acid
200 to the sampled air flow. Each background and calibration measurement period lasted ~4
201 and ~3.5 min, respectively, which not only gave the scrubber (during background
202 measurements) and flow tube ample time to equilibrate when the three-way PFA Teflon
203 valve was switched between ambient and background modes, but also allowed us to obtain
204 good averaging statistics during background and calibration measurements. A 1.12 ppm
205 ³⁴SO₂ gas standard was used as the source of the sulfur standard addition. 1.85 ppb of ³⁴SO₂
206 was added to sampled air flow during calibration measurements. The formic and acetic
207 acid calibration sources were permeation tubes (VICI Metronics) with emission rates of 91
208 and 110 ng min⁻¹, respectively. The emission rates were measured by scrubbing the output
209 of the permeation tube in deionized water via a gas impinger immersed in water, which
210 was then analyzed for formate and acetate using ion chromatography (Thermo Fisher
211 Scientific). Eight samples of each acid were analyzed over the course of the field study and
212 the standard deviations of the permeation rates were ≤ 6 %. 6.75 ppb of formic acid and
213 5.87 ppb of acetic acid was added to sampled air flow during calibration measurements.
214 The CIMS instrument sensitivity measured by the F₂³⁴SO₂⁻ ion signal (m/z 104) was
215 similarly applied to all the other measured species (except for formic and acetic acids)

216 using relative sensitivities determined in laboratory studies. The $F_2^{34}SO_2^-$ calibrant ion
217 signals were also used to calibrate ambient $F_2^{32}SO_2^-$ ion signals and determine ambient SO_2
218 concentrations as discussed in section 3.2.5.

219 2.2.3. Laboratory calibration

220 To estimate the levels of sensitivities for a series of acids of atmospheric relevance,
221 HNO_3 , oxalic, butyric, glycolic, propionic and valeric acid standard addition calibrations
222 were performed in post-field laboratory work. Many of these acids have previously been
223 measured in rural and urban environments (Kawamura et al., 1985; Veres et al., 2011;
224 Brophy and Farmer, 2015). The response of the CIMS acid signals were measured relative
225 to the sensitivity of $^{34}SO_2$ in these calibration measurements. The HNO_3 calibration source
226 was a permeation tube (KIN-TEK) with a permeation rate of 39 ng min^{-1} , which was
227 measured using UV optical absorption (Neuman et al., 2003). Solid or liquid samples of
228 oxalic (Sigma Aldrich, $\geq 99 \%$), butyric (Sigma Aldrich, $\geq 99 \%$), glycolic (Sigma Aldrich,
229 99%), propionic (Sigma Aldrich, $\geq 99.5 \%$) and valeric (Sigma Aldrich, $\geq 99 \%$) acids
230 were used in calibration measurements. The acid sample was placed in a glass impinger,
231 which was immersed in an ice bath to provide a constant vapor pressure. A flow of 6 to 10
232 mL min^{-1} of N_2 was passed over the organic acid in the glass impinger. This organic acid
233 air stream was then diluted with varying flows of N_2 (1 to 5 L min^{-1}) to achieve different
234 mixing ratios of the organic acid. Mixing ratios were calculated from either the acid's
235 emission rate from the impinger or the acid's vapor pressure. The emission rate of gas-
236 phase oxalic acid from the impinger was measured by scrubbing the output in deionized
237 water using the same method for calibrating the formic and acetic acid permeation tubes,
238 followed by ion chromatography analysis for oxalate. Three samples were analyzed and
239 the emission rate was determined to be 14 ng min^{-1} with a standard deviation of $< 5 \%$. The
240 vapor pressures of butyric and propionic acids at $0 \text{ }^\circ\text{C}$ were measured using a capacitance
241 manometer (MKS Instruments). The vapor pressures of glycolic and valeric acids at $0 \text{ }^\circ\text{C}$
242 were estimated using their literature vapor pressures at $25 \text{ }^\circ\text{C}$ and enthalpies of vaporization
243 (Daubert and Danner, 1989; Lide, 1995; Acree and Chickos, 2010).

244 Attempts to generate a calibration plot for pyruvic acid using its liquid sample
245 (Sigma Aldrich, 98%) and the setup described above were unsuccessful as this acid was

246 found to interact very strongly with surfaces. Glyoxylic acid calibrations were not
247 performed due to the presence of impurities in the glyoxylic acid monohydrate solution
248 used (Sigma Aldrich, 98 %), which resulted in the appearance of ions not attributed to
249 glyoxylic acid. We attempted to generate calibration plots for malonic (Sigma Aldrich, \geq
250 99.5 %), succinic (Sigma Aldrich, 99 %) and glutaric (Sigma Aldrich, 99 %) acids by
251 passing N₂ over their solid samples at room temperature. However, it was not possible to
252 generate large enough gas phase concentrations for calibration since these organic acids
253 have very low vapor pressures. The vapor pressures of malonic, succinic and glutaric acids
254 are 5.73×10^{-4} , 1.13×10^{-4} and 4.21×10^{-4} kPa at 298 K, respectively (Booth et al., 2010),
255 which are at least 2 orders of magnitude lower than the organic acids that we calibrated.
256 Although heating up the malonic, succinic and glutaric acid samples will likely generate
257 sufficient vapors for calibration, this method of generating calibrant gases will lead to large
258 measurement uncertainties due to vapors condensing out and adhering onto surfaces at
259 room temperature prior to introduction into the CIMS.

260 2.2.4. Detection limits and measurement uncertainties

261 The detection limits of the organic acids were estimated as 3 times the standard
262 deviation values (3σ) of the ion signals measured during background mode. Although each
263 background measurement period lasted ~ 4 min, ion signals of the different organic acids
264 took up to 1.5 min to stabilize during the switch between ambient, calibration and
265 background measurements during the field study. Thus, ion signals measured during the
266 first 1.5 min were not included in the calculation of the average and standard deviation of
267 ion signals measured during background mode. Table 1 summarizes the average detection
268 limits of calibrated organic acids for 2.5 min averaging periods which corresponds to the
269 length of a background measurement with a 4 % duty cycle for each m/z. The mean
270 difference between successive background measurements ranged from 1 to 40 ppt for the
271 different organic acids. Future work will focus on reducing the instrument background, and
272 therefore improving the detection limits of these organic acids.

273 The uncertainties (1σ) in our ambient measurements of formic, acetic and oxalic
274 acid concentrations originated from CIMS and ion chromatography, calibration
275 measurements. The ion chromatography measurement uncertainty was estimated to be 10

Deleted: the

Deleted: IC

Deleted: IC

279 % . For formic and acetic acids, which were calibrated during the field study using
280 permeation tubes, their CIMS measurement uncertainties were estimated to be 6 and 7 %,
281 respectively, based on one standard deviation of the acids' calibrant ion signals. For oxalic
282 acid, which was calibrated in post-field laboratory work, the CIMS measurement
283 uncertainty was estimated to be 9 % based on one standard deviation of the ³⁴SO₂
284 sensitivity (3 %), the acid's calibrant ion signals (7 %) and linear fit of the calibration curve
285 (5 %). Hence, the uncertainties in our ambient measurements of formic, acetic and oxalic
286 acid concentrations were estimated to be 12, 12 and 14 %, respectively.

287 For nitric acid, which was calibrated in post-field laboratory work using a
288 permeation tube and UV optical absorption, the uncertainty in its ambient concentrations
289 was estimated to be 13 % based on uncertainties in UV absorption measurements (10 %)
290 and one standard deviation of the acid's UV absorption signals (3 %), ³⁴SO₂ sensitivity (3
291 %) and acid's calibrant ion signals (8 %). For propionic acid, which was calibrated in post-
292 field laboratory work using vapor pressures measured by a capacitance manometer, the
293 uncertainty in its ambient concentrations was estimated to be 14 % based on the vapor
294 pressure measurement uncertainty (10 %) and one standard deviation of the ³⁴SO₂
295 sensitivity (3 %), the acid's calibrant ion signals (8 %) and linear fits of the acid's
296 calibration curves (3 %). **Ambient concentrations and the corresponding uncertainties of
297 glycolic, valeric and butyric acids were not quantified.**

298 2.3. WSOC_g measurements

299 WSOC_g was measured with a MIST chamber coupled to a total organic carbon
300 (TOC) analyzer (Sievers 900 series, GE Analytical Instruments). Ambient air first passed
301 through a Teflon filter (45 mm diameter, 2.0 μm pore size, Pall Life Sciences) to remove
302 particles in the air stream. This filter was changed every 3 to 4 days. The particle-free air
303 was then pulled into a glass Mist Chamber filled with ultrapure deionized water at a flow
304 rate of 20 L min⁻¹. The MIST chamber scrubbed soluble gases with Henry's law constants
305 greater than 10³ M atm⁻¹ into deionized water (Spaulding et al., 2002). The resulting liquid
306 samples from the MIST chamber were analyzed by the TOC analyzer. The TOC analyzer
307 converted the organic carbon in the liquid samples to carbon dioxide using UV light and
308 chemical oxidation. The carbon dioxide formed was then measured by conductivity. The

Deleted: butyric and

Deleted: s

Deleted: ere

Deleted: ies

Deleted: their

Deleted: ere

Deleted: '

Deleted: '

Deleted: For glycolic and valeric acids which were calibrated in post-field laboratory work using vapor pressures estimated from literature vapor pressures at 25 °C and enthalpies of vaporization, the uncertainties in their ambient concentrations were likely significantly larger compared to the other measured organic acids due to uncertainties in their estimated vapor pressures. We estimate the uncertainties in ambient concentrations of glycolic and valeric acids to be 22 % based on an assumed vapor pressure uncertainty of 20 % and one standard deviation of the ³⁴SO₂ sensitivity (3 %), the acids' calibrant ion signals (8 %) and linear fits of the acids' calibration curves (2 %).

329 amount of organic carbon in the liquid samples is proportional to the measured increase in
330 conductivity of the dissolved carbon dioxide. Each WSOC_g measurement lasted 4 min.
331 Background WSOC_g measurements were performed for 45 min every 12 h by stopping the
332 sample air flow and rinsing the sampling lines with deionized water. The TOC analyzer
333 was calibrated using different concentrations of sucrose (as specified by the instrument
334 manual) before and after the field study. The limit of detection was 0.4 µgC m⁻³. The
335 measurement uncertainty was estimated to be 10 % based on uncertainties in the sample
336 air flow, liquid flow and TOC analyzer uncertainty. The MIST chamber and upstream
337 particle filter were located in an air-conditioned building so were generally below ambient
338 temperature. Hence, evaporation of collected particles (which will lead to positive artifacts
339 in WSOC_g measurements) are not expected to be significant.

340 **2.4. Supporting gas measurements**

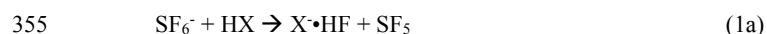
341 Supporting gas measurements were provided by a suite of instruments operated by
342 the SEARCH network. A non-dispersive infrared spectrometer (Thermo Fisher Scientific)
343 provided hourly CO measurements. A UV absorption analyzer (Thermo Fisher Scientific)
344 provided hourly O₃ measurements. A gas chromatography-flame ionization detector (GC-
345 FID, Agilent Technologies) provided hourly VOC measurements.

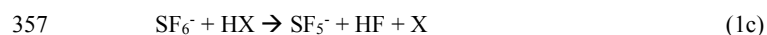
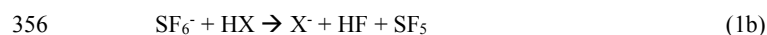
346 **3. Results and discussion**

347 **3.1. General SF₆⁻ CIMS field performance**

348 **3.1.1. SF₆⁻ ion chemistry with organic acids**

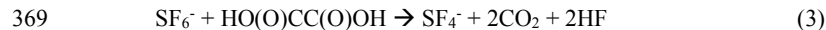
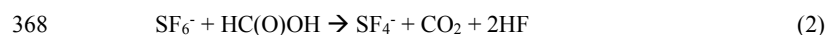
349 CIMS measurements of atmospheric constituents use ion-molecule reactions to
350 selectively ionize compounds of interest in the complex matrix of ambient air and produce
351 characteristic ions. The reactions of SF₆⁻ with the organic acids (HX) proceed through
352 reactions 1a to 1c, and gave similar products to those reported previously for SF₆⁻ reactions
353 with inorganic acids (Huey et al., 1995): SF₅⁻, X⁻ and X⁻•HF where X⁻ is the conjugate base
354 of the organic acid (reactions 1a-c).





358 The effective branching ratios of the SF_5^- , X^- and $\text{X} \cdot \text{HF}$ product ions can be impacted by
359 the field strength of the CDC. The SF_5^- ion (m/z 127, reaction 1c) is a common reaction
360 product of the reactions of SF_6^- with many species and is probably thermodynamically
361 driven by the formation of HF (Huey et al., 1995). Unfortunately, the production of SF_5^-
362 does not allow for the selective detection of any atmospheric species. In addition, the larger
363 the branching ratio of the SF_5^- channel, the lower the CIMS sensitivity is to an individual
364 acid since the effective rate constants for the X^- and $\text{X} \cdot \text{HF}$ channels are lower.

365 The reaction of SF_6^- with formic acid and oxalic acid also produced SF_4^- ions (m/z
366 108). These reactions are probably thermodynamically driven by the formation of CO_2 and
367 HF:



370 We used the X^- and/or $\text{X} \cdot \text{HF}$ ions to determine ambient organic acid concentrations
371 since these ions are characteristic of the individual acids. For all the organic acids, the X^-
372 $\cdot \text{HF}$ ion signal is substantially lower than that of the X^- ion for the conditions in this study.
373 However, this is probably largely due to the relatively high collision energy used in the
374 CDC_x which led to efficient dissociation of the fluoride adducts to form X^- ions.
375 Consequently, only the proton transfer channel (1b) is used to quantify most of the organic
376 acids in the field study. The exceptions are formic and acetic acid as discussed in section
377 3.2.1 and 3.2.2

378 Table 1 shows a summary of the sensitivities of X^- and $\text{X} \cdot \text{HF}$ ions of [some common](#)
379 [atmospheric](#) organic acids. The average sensitivities of the HCOO^- (m/z 45) and HCOO^-
380 $\cdot \text{HF}$ (m/z 65) ions of formic acid were 1.29 ± 0.22 and 0.29 ± 0.05 Hz ppt⁻¹, respectively,
381 while the average sensitivities of the CH_3COO^- (m/z 59) and $\text{CH}_3\text{COO}^- \cdot \text{HF}$ (m/z 79) ions
382 of acetic acid were 1.46 ± 0.29 and 0.30 ± 0.06 Hz ppt⁻¹, respectively. A weak ²¹⁰Po ion
383 source (< 1 mCi) was used by SF_6^- -CIMS instrument during the field study, hence these

384 sensitivities will be substantially higher if a stronger radioactive source is used. [Post-field](#)
385 [laboratory work suggest that the sensitivities may increase by as much as a factor of 5 for](#)
386 [a new commercial 20 mCi ²¹⁰Po ion source.](#) Nevertheless, these sensitivities are compared
387 to formic and acetic acid sensitivities measured by a high-resolution time-of-flight
388 chemical ionization mass spectrometer (Aerodyne Research Inc.) that utilized I⁻ reagent
389 ions during the field study. Although the formic acid sensitivity measured by I-CIMS (1.33
390 ± 0.28 Hz ppt⁻¹) was comparable to that measured by SF₆⁻-CIMS, the acetic acid sensitivity
391 measured by I-CIMS (< 0.1 Hz ppt⁻¹) was substantially lower than that measured by SF₆-
392 CIMS. Previous studies have similarly reported low acetic acid sensitivity measured by I-
393 CIMS (Aljawhary et al., 2013; Lee et al., 2014).

394 3.1.2. Characterization of interferences

395 SF₆⁻ is very sensitive to many trace atmospheric species but its reactions with water
396 vapor and O₃ when sampling ambient air can lead to issues both with selectivity and
397 stability. For example, SF₆⁻ reacts nonlinearly with water vapor to form a series of F•(HF)_n
398 cluster ions (Huey et al., 1995; Arnold and Viggiano, 2001). SF₆⁻ also reacts efficiently
399 with O₃ to form O₃⁻, which is rapidly converted to CO₃⁻ in ambient air (Slusher et al., 2001).
400 These reactions can deplete SF₆⁻ as well as form a variety of potentially interfering ions
401 from secondary reactions (e.g., F•(HF)_n and CO₃⁻ ions) that depend on more abundant
402 atmospheric species. For these reasons, efforts were made to minimize interferences by
403 limiting reaction times and the flow sampled into the CIMS. This was accomplished by
404 sampling only 0.3 L min⁻¹ of air through the variable orifice into the flow tube and
405 maintaining the flow tube at a low pressure (~13 mbar). The 0.3 L min⁻¹ sampled air flow
406 is diluted by 3.7 slpm of N₂/SF₆ flow in the flow tube. The ratio of the sampled air flow to
407 the N₂/SF₆ flow introduced into the flow tube is approximately 1:13. While the high N₂/SF₆
408 flow (3.7 slpm) passed through the radioactive source into the flow tube increased the SF₆⁻
409 reagent ion signal, the high dilution of the sampled air flow in the flow tube reduced the
410 CIMS instrument sensitivity by decreasing the number density of the analytes.

411 Figure 2 shows a mass spectrum of ambient air. Interference peaks at m/z 39 (F•
412 •(HF) and CO₃⁻, respectively) can be attributed to the presence of water and O₃,
413 respectively. The reagent ion ³²SF₆⁻ is present at m/z 146. The ³²SF₆⁻ reagent ion signal was

414 saturated, and this caused the sharp drop in the m/z 146 signal as shown in Fig. 2. Since
415 the $^{32}\text{SF}_6^-$ reagent ion signal was saturated for the entire field study, we monitored the ion
416 signal of its isotope $^{34}\text{SF}_6^-$ to determine if the reaction of SF_6^- with ambient water vapor
417 (5.92×10^{-6} to 2.19×10^{-5} g cm^{-3}) and O_3 (2.1 to 82.4 ppb) depleted SF_6^- reagent ions.
418 Figure S2a shows the time series of the $^{34}\text{SF}_6^-$ ion signal and ambient water vapor
419 concentration for the entire field study. Despite fluctuations in ambient water vapor and O_3
420 concentrations, the $^{34}\text{SF}_6^-$ ion signal was relatively constant for the entire field study with
421 a standard deviation of $< 3\%$. This indicates that the reaction of SF_6^- with ambient water
422 vapor and O_3 did not significantly deplete the $^{32}\text{SF}_6^-$ reagent ions during the field study.

423 The $\text{F}_2^{34}\text{SO}_2^-$ ion signal was used to monitor the CIMS SO_2 sensitivity during the
424 field study. Figure S2b shows the time series of the $\text{F}_2^{34}\text{SO}_2^-/^{34}\text{SF}_6^-$ ion signal ratio obtained
425 in calibration measurements. There is a $\sim 50\%$ increase in the $\text{F}_2^{34}\text{SO}_2^-/^{34}\text{SF}_6^-$ ion signal
426 ratio on 28 Sept 2016, indicating an increase in the CIMS instrument sensitivity. The
427 increase in CIMS instrument sensitivity is due to the decrease in ambient water vapor
428 concentrations on 28 Sept 2016 (Fig. S2a). Previous laboratory and field studies showed
429 that this was due to the hydrolysis of $\text{F}_2^{34}\text{SO}_2^-$, which led to the loss of this ion and
430 diminished sensitivity at higher levels of ambient water vapor (Arnold and Viggiano, 2001;
431 Slusher et al., 2001). However, the SO_2 sensitivity at $\text{F}_2^{34}\text{SO}_2^-$ only varied within a factor
432 of two for the entire field study with a clear relationship to water vapor (Fig. S2c). The SO_2
433 sensitivity did not show any obvious dependence on ambient O_3 concentrations (Fig. S2d).

434 The formic (HCOO^- at m/z 45 and $\text{HCOO}\cdot\text{HF}$ at m/z 65) and acetic (CH_3COO^-
435 $\cdot\text{HF}$ at m/z 79) acid ions did not show any obvious dependence on ambient water vapor
436 and O_3 concentrations during calibration measurements (Fig. S3). Therefore, we do not
437 expect the sensitivities of the X^- and $\text{X}\cdot\text{HF}$ ions of the studied organic acids to depend on
438 ambient water vapor and O_3 concentrations. We accounted for water vapor dependence of
439 the $\text{F}_2^{34}\text{SO}_2^-$ ion signal using the linear relationship between the $\text{F}_2^{34}\text{SO}_2^-$ ion sensitivity
440 and ambient water vapor concentration (Fig. S2c) in our post-field calibrations, where the
441 response of the CIMS acid signals were measured relative to the of the $^{34}\text{SO}_2$ sensitivity.

442 3.1.3. Background and calibration measurements

Deleted: noticeable

444 Figure S4 shows an example of the CIMS instrument response during the switch
445 between background, calibration and ambient measurements of formic and acetic acids
446 during the field study. The 13 s time resolution data was used to determine the CIMS
447 instrument time response. Formic (m/z 45, 65 and 108) and acetic (m/z 79) acid ion signals
448 took ~1.5 min to reach a steady state after switches between ambient, calibration and
449 background measurements (Figs. S4a and S4c).

450 The CIMS time response to a compound is governed primarily by the compound's
451 propensity to adhere to surfaces. The decays in the formic and acetic acid ion signals and
452 times required for them to reach steady state after the removal of calibration gases during
453 the switch from standard addition calibration to ambient sampling were used to determine
454 the CIMS response time. The signal decays were fitted using double exponential functions.
455 For formic acid, the m/z 45, 65 and 108 ion signals decayed to $1/e^2$ in 37 ± 2 , 33 ± 2 and
456 32 ± 2 s, respectively (Fig. S4b). For acetic acid, the m/z 79 ion signal decayed to $1/e^2$ in
457 42 ± 2 s (Fig. S4d).

Formatted: Level 1

458 3.2. Ambient measurements

459 3.2.1. Formic acid

460 Figure 2 shows typical mass spectra obtained under background and measurement
461 modes during the field study. The SF_6^- reagent ion is present at m/z 146. One of the
462 prominent species in the mass spectrum is formic acid, which is detected as HCOO^- and
463 $\text{HCOO}\cdot\text{HF}$ at m/z 45 and 65, respectively. Our laboratory studies demonstrated that the
464 reaction of formic acid with SF_6^- also produced a large fraction of SF_4^- ions at m/z 108.
465 The reaction of SF_6^- with oxalic acid also produced SF_4^- ions, but its SF_4^- product ion yield
466 is low and gas phase oxalic acid is not present in large concentrations. In addition, SF_4^- is
467 present in the mass spectrum obtained under background mode but the SF_4^- background
468 ion signals are lower than those typically observed in measurement mode at the Yorkville
469 site. As a result, we determined the ambient formic acid concentrations using the HCOO^- ,
470 $\text{HCOO}\cdot\text{HF}$ and SF_4^- ions. Figure 3a shows a scatter plot comparing the ambient formic
471 acid concentrations measured at Yorkville using the HCOO^- , $\text{HCOO}\cdot\text{HF}$ and SF_4^- ions.
472 Linear regression analysis reveals that the formic acid concentrations determined by the

473 three ions are highly correlated ($R^2 = 0.99$) with slopes exhibiting a near 1:1 correlation.
474 The excellent correlation between these three ions and the agreement with laboratory data
475 indicates that formic acid is selectively measured by this method.

476 The time series of formic acid, temperature and solar radiation measured at
477 Yorkville are shown in Fig. 3b. Formic acid concentrations ranged from 40 ppt to 4 ppb
478 during the field study, with strong and consistent diurnal trends. The day-to-day variability
479 in formic acid concentrations are associated with changes in solar radiation and
480 temperature. Higher formic acid concentrations are measured during warm and sunny days,
481 similar to formic acid measurements performed in Centreville, rural Alabama during the
482 2013 Southern Oxidant Aerosol Study (SOAS) (Brophy and Farmer, 2015; Millet et al.,
483 2015). Figure 3c shows the study-averaged diurnal profiles of formic acid and solar
484 irradiance. Formic acid started to increase at 7:30, which coincided with a sharp increase
485 in solar irradiance. Concentrations continued to increase throughout the day and peaked at
486 18:30, which coincided with the approximate time just before solar irradiance reached zero.
487 Formic acid then decreased continuously throughout the night.

488 The immediate early-morning increase in formic acid observed in this field study
489 is similar to that seen during the SOAS study (Millet et al., 2015). However, there are some
490 differences in the formic acid diurnal cycles measured in this field study and the SOAS
491 study. Formic acid peaked at 15:30 during SOAS, approximately 3 hours before solar
492 irradiance decreased to zero. In contrast, formic acid concentrations only started to
493 decrease at sunset (at 19:30) in this study. This suggests that there may be differences in
494 the types and/or magnitudes of formic acid sources and sinks in this two field studies. Land
495 cover and/or land use differences may have contributed to differences in formic acid
496 sources and sinks at the Centreville and Yorkville field sites. The area surrounding the
497 Yorkville field site is covered primarily by hardwood mixed with farmland and open
498 pastures. In contrast, the Centreville field site is surrounded by forests comprised of mixed
499 oak-hickory and loblolly trees (Hansen et al., 2003). It is also possible that seasonal
500 differences contributed to differences in formic acid sources and sinks in the two field
501 studies. The SOAS campaign took place in the middle of summer (1 June to 15 July 2013)
502 when biogenic emissions are typically higher while this field study took place in early fall

503 when biogenic emissions are lower due to cooler temperatures. For example, the average
504 concentration of isoprene (a formic acid source) in this study (1.21 ppb) is lower than that
505 in SOAS (1.92 ppb (Millet et al., 2015)). Despite these differences, our overall results are
506 similar to the formic acid measurements performed in SOAS in both magnitude and diurnal
507 variability.

508 3.2.2. Acetic acid

509 Acetic acid is detected with SF_6^- as CH_3COO^- and $\text{CH}_3\text{COO}^-\cdot\text{HF}$ at m/z 59 and 79,
510 respectively. However, these ions are subject to interferences from the reaction of SF_6^- with
511 water vapor present in the sampled ambient air. Two of these interfering ions $\text{F}^-\cdot(\text{HF})_2$ and
512 $\text{F}^-\cdot(\text{HF})_3$ occur at m/z 59 and 79, respectively. As discussed earlier, we minimized the
513 impact of these interferences by diluting the sample flow into the CIMS and running the
514 CDC at a high collision energy to dissociate the HF cluster ions. As expected from cluster
515 bond strengths, we found that larger HF cluster ions dissociated more easily than smaller
516 ones. For example, at a CDC electric field of $\sim 113 \text{ V cm}^{-1}$ (the configuration used in this
517 field study), virtually all of the $\text{F}^-\cdot(\text{HF})_3$ cluster ions dissociated while very few of the $\text{F}^-\cdot$
518 (HF) cluster ions dissociated. This indicates that the m/z 79 channel for acetic acid is more
519 immune to interference from water vapor than the m/z 59 channel. This is supported by the
520 observation that the background ion signal at m/z 59 ($R^2 = 0.50$) is more highly correlated
521 with ambient water vapor concentrations than the background ion signal of m/z 79 ($R^2 =$
522 0.30). In addition, the m/z 59 ion is subjected to interference from the reaction of SF_6^- with
523 O_3 present in the sampled ambient air. SF_6^- reacts with O_3 in the presence of CO_2 to form
524 CO_3^- at m/z 60 (Slusher et al., 2001). As shown in Fig. 2, the large CO_3^- peak at m/z 60 is
525 a potential interference to the m/z 59 signal. As the background scrubber also removed O_3
526 from the ambient air, there is a large difference in the m/z 60 ion signal between the
527 measurement and background modes ($\sim 100,000 \text{ Hz}$). Thus, even a few percent bleed over
528 of m/z 60 to m/z 59 can lead to an over-estimation of ambient acetic acid concentrations.
529 For these reasons, we used m/z 79 ($\text{X}^-\cdot\text{HF}$) to determine ambient acetic acid concentrations
530 even though this channel has a lower sensitivity than the m/z 59 channel (X^-).

531 The time series of acetic acid, temperature and solar radiation measured at
532 Yorkville are shown in Fig. 4a. Acetic acid concentrations ranged from 30 ppt to 3 ppb

Deleted: ,

534 during the field study. The day-to-day variability in acetic acid concentrations resembled
535 the behavior of formic acid concentrations, with higher concentrations being measured
536 during warm and sunny days. Figure 4b shows the study-averaged diurnal profiles of acetic
537 acid and solar irradiance. The diurnal profile of acetic acid is similar to that of formic acid
538 with a more pronounced evening maximum. Acetic acid started to increase at 7:30 and
539 built up through the day, peaking at 19:30 and decreased continuously overnight. In
540 general, acetic acid concentrations are well correlated with ($R^2 = 0.67$) and comparable in
541 magnitude (~60 % on average) to formic acid. The study-averaged formic acid/acetic acid
542 concentration ratio (1.65) is comparable to ratios from previous field studies in rural and
543 urban environments (Talbot et al., 1988; Talbot et al., 1995; Granby et al., 1997; Khare et
544 al., 1999; Talbot et al., 1999; Baboukas et al., 2000; Singh et al., 2000; Kuhn et al., 2002;
545 Baasandorj et al., 2015; Millet et al., 2015).

546 3.2.3. Larger organic acids

547 In addition to formic and acetic acid, eight other ions were monitored during the
548 field study: m/z 73, 75, 87, 89, 101, 103, 117 and 131. These ions were chosen as they had
549 significant signals when ambient air was sampled and were not obviously formed from
550 SF_6^- reaction with water vapor or O_3 . Since the CIMS utilized in this study only had unit
551 mass resolution, these ions are the sum of all organic acid isomers and isobaric organic
552 acids of the same molecular weight as well as other product ions from species that might
553 react with SF_6^- . We will refer to organic acids with m/z 75, 87, 101, 103, 117 and 131 by
554 their ion masses. We assign the m/z 73 ion as the X^- ion of propionic acid because it does
555 not have organic acid isomers and isobaric species at that m/z . In addition, real-time ion
556 chromatography measurements of aerosol composition performed during the field study
557 demonstrated the presence of particulate oxalic acid (Nah et al., 2018). For this reason, we
558 assign the m/z 89 ion as the X^- ion of oxalic acid. As shown in Nah et al. (2018), the gas-
559 particle ratios of the organic acids depend of their thermodynamic conditions, which are
560 dependent on the acid's physicochemical properties, ambient temperature, particle water
561 and pH. Since the measured gas-particle partitioning ratios of oxalic acid (calculated using
562 the CIMS and ion chromatography measurements) are in good agreement with their
563 corresponding thermodynamic predictions (Nah et al., 2018), this indicated that our

Deleted: acid

Formatted: Level 1

Deleted: However, r

Deleted: ,

Deleted: malonic, succinic and glutaric

Deleted: s

Deleted: for

Deleted: ,

Deleted: 103, 117 and 131

Deleted: s,

Deleted: we assigned them

Deleted: s

Deleted: ,

Deleted: malonic, succinic and glutaric

Deleted: s, respectively

578 assignment of the m/z 89 ion to oxalic acid is reasonable. In addition, the high sensitivity
579 of SF₆ to oxalic acid also helps limit interferences due to other acids. Particulate formic
580 acid and acetic acid were also detected by ion chromatography during the field study, but
581 were at much lower concentrations relative to the gas phase (Nah et al., 2018).

582 Figures 5 and S5 show the time series and diurnal profiles of oxalic and propionic
583 acids and organic acids with ions m/z 75, 87, 101, 103, 117 and 131 measured during the
584 field study. These organic acids displayed very similar day-to-day variability as formic and
585 acetic acids, with higher concentrations (or ion signals) being measured on warm and sunny
586 days. The diurnal profiles of all the measured organic acids have similar diurnal trends,
587 with their concentrations (or ion signals) reaching a maximum between 17:30 and 19:30
588 and rapidly decreasing after sunset.

589 3.2.4. Comparison with WSOC_g

590 WSOC_g measurements were performed during the field study using a MIST
591 chamber coupled to a TOC analyzer. The study average WSOC_g was $3.6 \pm 2.7 \mu\text{gC m}^{-3}$,
592 slightly lower than that measured during the SOAS study ($4.9 \mu\text{gC m}^{-3}$) (Xu et al., 2017),
593 and approximately four times lower than that measured in urban Atlanta, Georgia (13.7
594 $\mu\text{gC m}^{-3}$) (Hennigan et al., 2009). Despite being comparable in magnitude, the diurnal
595 profiles of WSOC_g measured in this study and the SOAS study are different. WSOC_g
596 measured in the SOAS study decreased at sunset, while WSOC_g measured in this study
597 decreased 2 hours after sunset. Differences in WSOC_g concentrations and diurnal profiles
598 at the three different sites may be due to differences in emission sources as a result of
599 different measurement periods, land use and/or land cover.

600 To estimate the fraction of WSOC_g that is comprised of organic acids, the total
601 organic carbon contributed by formic, acetic, oxalic and propionic acids is compared to the
602 WSOC_g measurements. This comparison primarily serves as a check to determine if the
603 peak assignments are plausible by ensuring that the estimated sum of organic carbon
604 contributed by these four organic acids is less than or equal to the measured WSOC_g.
605 Figures 6a and 6b show the time series and diurnal profiles of WSOC_g and the organic
606 carbon contributed by the four organic acids. Formic and acetic acids comprised majority

Deleted: As these organic acids have low vapor pressures, their gas-phase concentrations are expected to be lower than their particle-phase concentrations, though their gas-particle ratios will depend on thermodynamic conditions (Nah et al., 2018).

Deleted: For simplicity, we also denoted m/z 73, 75, 87 and 101 ions as X⁻ ions of propionic, glycolic, butyric and valeric acids, respectively, for the remainder of this paper. These organic acids have previously been measured in rural and urban environments (Kawamura et al., 1985; Veres et al., 2011; Brophy and Farmer, 2015). However, we note that these assignments are speculative. Post-field calibration measurements were used to estimate the ambient concentrations of these organic acids.

Deleted: s

Deleted: ,

Deleted: butyric, glycolic, propionic and valeric acids

Deleted: Daytime concentrations of these organic acids ranged from a few tens of ppt to several hundred ppt. The time series of ion signals (Hz) of malonic, succinic and glutaric acids normalized to the instrument's sensitivity to F₂³⁴SO₂ (Hz ppb⁻¹) are shown in Fig. S3. The ion signals of these organic acids are 1 to 2 orders of magnitude smaller than the sensitivity of the F₂³⁴SO₂ ion (study-averaged sensitivity = $2928 \pm 669 \text{ Hz ppb}^{-1}$), resulting in these ratios to be less than 1. Concentrations of these organic acids are not available since calibrations were not performed for these compounds.

Deleted: eight

Deleted: ,

Deleted: butyric, glycolic,

Deleted: and valeric

Deleted: We emphasize that the ion peak assignment of some of these organic acids are speculative. Hence, t

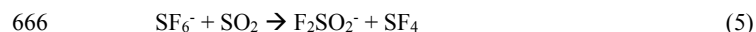
Deleted: zeroth order

Deleted: measured

643 of the total organic carbon contributed by the four organic acids (study averages of 41 and
 644 54%, respectively). The carbon mass fraction of WSOC_g comprised of these four organic
 645 acids ranged from 2 to 100%. Based on the orthogonal distance regression slope shown in
 646 Fig. 6c, the study-averaged carbon mass fraction of WSOC_g comprised of the four organic
 647 acids is 22%. The total organic carbon contributed by the four organic acids are moderately
 648 correlated with WSOC_g ($R^2 = 0.42$). This is likely due to the presence of other water-soluble
 649 gas phase species (with different day-to-day variability from the organic acids) that
 650 contribute to the WSOC_g. This is supported by slight differences in the diurnal profiles of
 651 WSOC_g and the organic carbon contributed by the organic acids (Fig. 6b). While the
 652 diurnal profiles of WSOC_g and the organic carbon contributed by the four organic acids
 653 have similar general shapes, WSOC_g peaked at 21:30, approximately 2 hours after the solar
 654 irradiance have decreased to zero. In contrast, the organic carbon contributed by the four
 655 organic acids start to decrease at sunset (at 19:30).

656 3.2.5. SO₂ and HNO₃ observations

657 In addition to evaluating the field performance of the SF₆⁻ CIMS technique in gas-
 658 phase organic acid measurements, another focus of this study was to investigate the
 659 possible sources of the measured organic acids. For this reason, HNO₃ and SO₂ (two
 660 common anthropogenic tracers) were also measured by SF₆⁻ CIMS during the field study.
 661 Correlations between the concentrations of organic acids and those of HNO₃ and SO₂ were
 662 then examined to determine if the organic acids were anthropogenic in nature (section 3.3).
 663 While their reactions with SF₆⁻ have multiple product channels (Huey et al., 1995), only
 664 the NO₃⁻•HF (m/z 82) and F₂SO₂⁻ (m/z 102) ions were used for quantitative purposes:



667 Figure S6 shows the time series of SO₂ and HNO₃ measured during the field study.
 668 As expected at a rural site, SO₂ and HNO₃ concentrations are low most of the time (study
 669 averages of 230 and 180 ppt, respectively). However, there were occasional periods when
 670 the site was impacted by anthropogenic pollution. In particular, there are spikes in both
 671 SO₂ and HNO₃ concentrations lasting between 1 to 3 hours throughout the study that

Deleted: measured

Deleted: 31

Formatted: Not Highlight

Deleted: 38

Deleted: Assuming that the ion peak assignments are correct and the measured organic acids are completely water-soluble, t

Deleted: 7

Formatted: Not Highlight

Deleted: measured

Deleted: 30

Deleted: measured

Deleted: 0.38

Deleted: S4

684 corresponded to the site being impacted by power plant or urban emissions. Outside of
685 these anthropogenic spikes, HNO₃ showed a clear diurnal profile with a maximum at
686 approximately 12:30, consistent with local photochemical production.

687 3.3. Potential sources of organic acids

688 Correlation analysis on organic acid concentrations can provide insights on their
689 sources. Figure 7 shows that the concentration of formic acid is strongly correlated with
690 those of the other measured organic acids ($R^2 = 0.68$ to 0.89). This suggests that these
691 organic acids have the same or similar sources at Yorkville. The sources of organic acids
692 can be biogenic or anthropogenic in nature. To determine if the primary sources of organic
693 acids are of biogenic or anthropogenic origin, we first examined the correlations of organic
694 acid concentrations with those of anthropogenic pollutants CO, SO₂, O₃ and HNO₃. CO
695 and SO₂ are common tracers for combustion sources. The organic acid concentrations (or
696 ion signals) are poorly correlated with CO (Fig. S7, $R^2 = 0.04$ to 0.15) and SO₂ (Fig. S8,
697 $R^2 = 0.01$ to 0.23), indicating that primary emissions from combustion are a minor source
698 of organic acids in Yorkville. HNO₃ and O₃ are common photochemical tracers of urban
699 air masses. The organic acid concentrations (or ion signals) are weakly correlated with O₃
700 (Fig. S9, $R^2 = 0.11$ to 0.31) and HNO₃ (Fig. S10, $R^2 = 0.33$ to 0.60). In addition, there is
701 no noticeable increase in organic acid concentrations during periods of elevated CO, SO₂,
702 O₃ and HNO₃ concentrations when the site was impacted by pollution plumes. Formic
703 acid/CO ratios (which have been used in some studies to determine the contribution of
704 polluted air masses) ranged between 1.0×10^{-3} to 2.5×10^{-2} ppb ppb⁻¹. The ratio peaked
705 consistently in the mid-afternoon, which coincided with when formic acid and CO reached
706 their maximum and minimum, respectively. In addition, there were no spikes in the formic
707 acid/CO ratio during the study, suggesting that contributions of polluted air masses to the
708 daily increase in formic acid are minimal. Together, these results indicate that the primary
709 sources of organic acids in Yorkville are likely not anthropogenic in nature.

710 Diurnal profiles of the measured organic acids suggest that their sources are linked
711 to higher daytime temperatures and/or photochemical processes. Figure 8 compares the
712 concentrations (or ion signals) of organic acids against ambient temperatures measured
713 during the study. Since there was a noticeable decrease in mean ambient temperatures

Deleted: 5

Deleted: 03

Deleted: S6

Deleted: 24

Deleted: S7

Deleted: 32

Deleted: S8

Deleted: 5

722 starting on 28 Sept 2016, we grouped the datasets into two time periods (3 to 27 Sept and
723 28 Sept to 12 Oct) to better evaluate the effect of temperature on organic acid
724 concentrations. The average temperature in the first time period (3 to 27 Sept) is 24.8 °C
725 (32.6 °C max, 18.1 °C min), while the average temperature in the second time period (28
726 Sept to 12 Oct) is 19.5 °C (28.4 °C max, 9.5 °C min). We find that organic acid
727 concentrations are on average higher and more highly correlated with temperatures in the
728 warmer first time period ($R^2 = 0.40$ to 0.61) compared to the cooler second time period (R^2
729 $= 0.18$ to 0.55). These observations can be explained by temperature-dependent emissions
730 of organic acids and their BVOC precursors. Previous studies have shown that emissions
731 of organic acids and their BVOC precursors depend strongly on light and temperature, with
732 substantially lower concentrations being emitted in the dark and/or at low temperatures
733 (Kesselmeier et al., 1997; Kesselmeier, 2001; Sindelarova et al., 2014). We find that the
734 concentration of isoprene, which was the dominant BVOC in Yorkville, has a somewhat
735 similar diurnal profile as the organic acids and decreased with temperature on 28 Sept 2016
736 (Fig. [S11](#)). In addition, the concentrations of formic and acetic acids are moderately
737 correlated with that of isoprene ($R^2 = 0.42$ and 0.40 , respectively) (Fig. [S12](#)).

Deleted: 63

Deleted: 59

Deleted: S9

Deleted: S10

738 Multiphase photochemical aging of ambient organic aerosols can also be a source
739 of gas-phase organic acids (Eliason et al., 2003; Ervens et al., 2004; Molina et al., 2004;
740 Lim et al., 2005; Park et al., 2006; Walser et al., 2007; Sorooshian et al., 2007; Vlasenko
741 et al., 2008; Pan et al., 2009; Sorooshian et al., 2010). Organic acids may be formed in the
742 particle phase during organic aerosol photochemical aging, with subsequent volatilization
743 into the gas phase. Real-time ion chromatography measurements of aerosol composition
744 demonstrated the presence of particulate formic, acetic, oxalic, malonic, succinic and
745 glutaric acids (Nah et al., 2018). However, since the ratios of gas-phase formic and acetic
746 acid mass concentration to the total organic aerosol mass concentration are large (study
747 averages of 40 and 35 %, respectively) (Nah et al., 2018), it is unlikely that organic aerosol
748 photochemical aging is a large source of formic and acetic acids. In contrast, the ratios of
749 gas-phase oxalic, malonic, succinic and glutaric acids mass concentration to the total
750 organic aerosol mass concentration are expected to be small, suggesting that organic
751 aerosol photochemical aging may be an important source of these gas-phase organic acids.

756 In summary, the temperature dependence and diurnal profile of organic acid
757 concentrations combined with poor correlations between organic acid concentrations and
758 those of anthropogenic pollutants CO, SO₂, O₃ and HNO₃ strongly suggest that the primary
759 sources of gas-phase organic acids at Yorkville are biogenic in nature. However, our data
760 alone does not allow us to determine if the organic acids are a result of direct emissions or
761 photochemical oxidation of other BVOC emissions and/or organic aerosols. Partitioning
762 of these organic acids between the gas and particle phases ~~is discussed in another paper~~
763 (Nah et al., 2018).

Deleted: will b

Deleted: e

Deleted: forthcoming

764 4. Summary

765 SF₆⁻ reacted with all of the studied organic acids to produce product ions that were
766 characteristic of the individual acids (i.e., X⁻ or X•HF). These reactions all occurred at less
767 than the maximum collisional rate due to significant yields of SF₅⁻ and SF₄⁻, which reduced
768 the sensitivity of the method. For the conditions employed in this study, the sensitivities of
769 X⁻ and X•HF ions of the organic acids ~~ranged from 0.12 to 6.38 Hz ppt⁻¹~~. The detection
770 limits of the organic acids were approximated from 3 times the standard deviation values
771 (3σ) of the ion signals obtained during background measurements. Limits of detection
772 ranged from 1 to 60 ppt for 2.5 min integration periods for the organic acids studied. ~~It~~
773 ~~should be noted that the SF₆⁻ CIMS method is particularly sensitive to oxalic, propionic~~
774 ~~and glycolic acids, which are expected to be present at low concentrations in the~~
775 ~~atmosphere.~~ Water vapor and O₃ can lead to interferences with this method but for the
776 conditions employed in this study, they were largely limited to acetic acid measurements
777 at m/z 59. However, fluctuations in ambient water vapor can also lead to changes in
778 sensitivity for the detection of some species (e.g., SO₂). Uncertainties in organic acid
779 concentrations originate primarily from calibration measurements and ranged from ~~12~~ to
780 ~~14~~ %. Overall, the tractable mass spectra obtained by the SF₆⁻ CIMS method coupled with
781 reasonable limits of detection and the high correlations observed between the individual
782 organic acids demonstrated the potential of this method. Obvious next steps for the SF₆⁻
783 CIMS method are to compare it to other measurement methods for organic acids and to
784 deploy the SF₆⁻ ion chemistry to a higher resolution time-of-flight mass spectrometer to
785 reduce the potential for interferences.

Deleted: relative to that of the F₂³⁴SO₂⁻ ion (study-averaged sensitivity 2928 ± 669 Hz ppb⁻¹)

Deleted: 04

Deleted: 2.18

Deleted: Reasonable limits of detection for 2.5 min integration periods (1 to 60 ppt) were obtained for all the organic acids studied.

Deleted: 9

Deleted: 22

798 The SF₆ CIMS method was deployed for measurements of gas phase organic acids
799 in a mixed forest-agricultural area in Yorkville, Georgia from Sept to Oct 2016. The
800 organic acids measured in the field study were formic, acetic, propionic and oxalic acids.
801 Ambient concentrations of these organic acids ranged from a few ppt to several ppb. All
802 the organic acids exhibited similar strong diurnal trends. Organic acid concentrations built
803 up throughout the day, peaked between 17:30 and 19:30 before decreasing continuously
804 overnight. Strong correlations between organic acid concentrations indicated that these
805 organic acids likely have the same or similar sources at Yorkville. We concluded that the
806 organic acids were likely not due to anthropogenic emissions since they were poorly
807 correlated with anthropogenic pollutants and their concentrations were not elevated when
808 the site was impacted by pollution plumes. Higher organic acid concentrations were
809 measured during warm and sunny days. Organic acid concentrations were strongly
810 correlated with temperature during the first month of the study when ambient temperatures
811 were high. Together, our results suggested that the primary sources of organic acids at
812 Yorkville were biogenic in nature. Direct biogenic emissions of organic acids and/or their
813 BVOC precursors were likely enhanced at high ambient temperatures, resulting in the
814 observed variability of organic acid concentrations. Another potential source is the
815 production of organic acids in the particle phase from the multiphase photochemical aging
816 of organic aerosols followed by evaporation to the gas phase, though this source is likely
817 not a large source of formic and acetic acids. However, given the inability of current models
818 and photochemical mechanisms to explain formic acid observations in the Southeastern
819 U.S. (Millet et al., 2015), it is unlikely that our observations of formic acid and larger
820 organic acids can be explained as well. Further work (i.e., laboratory, field and modeling
821 studies) is needed to determine how organic acids are formed in the atmosphere.

822 5. Acknowledgements

823 The authors thank Eric Edgerton (Atmospheric Research and Analysis, Inc.) for
824 providing CO, O₃ and VOC measurements and meteorological data.

825 6. Funding

Deleted: and

Deleted: In addition, measurements tentatively assigned to oxalic, butyric, glycolic, propionic, valeric, malonic, succinic and glutaric acids were performed.

830 This publication was developed under US Environmental Protection Agency (EPA)
831 STAR Grant R835882 awarded to Georgia Institute of Technology. It has not been
832 formally reviewed by the EPA. The views expressed in this document are solely those of
833 the authors and do not necessarily reflect those of the EPA. EPA does not endorse any
834 products or commercial services mentioned in this publication.

835 **7. Competing financial interests**

836 The authors declare no competing financial interests.

837 **8. Data availability**

838 Data can be accessed by request (greg.huey@eas.gatech.edu).

839 **9. References**

840 Acree, W., and Chickos, J. S.: Phase Transition Enthalpy Measurements of Organic and
841 Organometallic Compounds. Sublimation, Vaporization and Fusion Enthalpies From 1880
842 to 2010, *J. Phys. Chem. Ref. Data*, 39, 942, 10.1063/1.3309507, 2010.

843 Aljawhary, D., Lee, A. K. Y., and Abbatt, J. P. D.: High-resolution chemical ionization
844 mass spectrometry (ToF-CIMS): application to study SOA composition and processing,
845 *Atmospheric Measurement Techniques*, 6, 3211-3224, 10.5194/amt-6-3211-2013, 2013.

846 Andreae, M. O., Talbot, R. W., Andreae, T. W., and Harriss, R. C.: Formic and Acetic
847 Acid over the Central Amazon Region, Brazil. 1. Dry Season, *Journal of Geophysical
848 Research-Atmospheres*, 93, 1616-1624, 10.1029/JD093iD02p01616, 1988.

849 Arnold, S. T., and Viggiano, A. A.: Turbulent ion flow tube study of the cluster-mediated
850 reactions of SF₆- with H₂O, CH₃OH, and C₂H₅OH from 50 to 500 torr, *J. Phys. Chem.
851 A*, 105, 3527-3531, 10.1021/jp003967y, 2001.

852 Baasandorj, M., Millet, D. B., Hu, L., Mitroo, D., and Williams, B. J.: Measuring acetic
853 and formic acid by proton-transfer-reaction mass spectrometry: sensitivity, humidity
854 dependence, and quantifying interferences, *Atmospheric Measurement Techniques*, 8,
855 1303-1321, 10.5194/amt-8-1303-2015, 2015.

856 Baboukas, E. D., Kanakidou, M., and Mihalopoulos, N.: Carboxylic acids in gas and
857 particulate phase above the Atlantic Ocean, *Journal of Geophysical Research-*
858 *Atmospheres*, 105, 14459-14471, 10.1029/1999jd900977, 2000.

859 Booth, A. M., Barley, M. H., Topping, D. O., McFiggans, G., Garforth, A., and Percival,
860 C. J.: Solid state and sub-cooled liquid vapour pressures of substituted dicarboxylic acids
861 using Knudsen Effusion Mass Spectrometry (KEMS) and Differential Scanning
862 Calorimetry, *Atmos. Chem. Phys.*, 10, 4879-4892, 10.5194/acp-10-4879-2010, 2010.

863 Brophy, P., and Farmer, D. K.: A switchable reagent ion high resolution time-of-flight
864 chemical ionization mass spectrometer for real-time measurement of gas phase oxidized
865 species: characterization from the 2013 southern oxidant and aerosol study, *Atmospheric*
866 *Measurement Techniques*, 8, 2945-2959, 10.5194/amt-8-2945-2015, 2015.

867 Carlton, A. G., Turpin, B. J., Lim, H. J., Altieri, K. E., and Seitzinger, S.: Link between
868 isoprene and secondary organic aerosol (SOA): Pyruvic acid oxidation yields low volatility
869 organic acids in clouds, *Geophys. Res. Lett.*, 33, 4, 10.1029/2005gl025374, 2006.

870 Chebbi, A., and Carlier, P.: Carboxylic acids in the troposphere, occurrence, sources, and
871 sinks: A review, *Atmospheric Environment*, 30, 4233-4249, 10.1016/1352-
872 2310(96)00102-1, 1996.

873 Crounse, J. D., McKinney, K. A., Kwan, A. J., and Wennberg, P. O.: Measurement of gas-
874 phase hydroperoxides by chemical ionization mass spectrometry, *Analytical Chemistry*,
875 78, 6726-6732, 10.1021/ac0604235, 2006.

876 Daubert, T. E., and Danner, R. P.: Physical and thermodynamic properties of pure
877 chemicals: data compilation, Taylor & Francis, Washington, DC, 1989.

878 Eliason, T. L., Aloisio, S., Donaldson, D. J., Cziczo, D. J., and Vaida, V.: Processing of
879 unsaturated organic acid films and aerosols by ozone, *Atmospheric Environment*, 37, 2207-
880 2219, 10.1016/s1352-2310(03)00149-3, 2003.

881 Ervens, B., Feingold, G., Frost, G. J., and Kreidenweis, S. M.: A modeling study of aqueous
882 production of dicarboxylic acids: 1. Chemical pathways and speciated organic mass

883 production, *Journal of Geophysical Research-Atmospheres*, 109, 10.1029/2003jd004387,
884 2004.

885 Ervens, B., Carlton, A. G., Turpin, B. J., Altieri, K. E., Kreidenweis, S. M., and Feingold,
886 G.: Secondary organic aerosol yields from cloud-processing of isoprene oxidation
887 products, *Geophys. Res. Lett.*, 35, 10.1029/2007gl031828, 2008.

888 Galloway, J. N., Likens, G. E., Keene, W. C., and Miller, J. M.: The Composition of
889 Precipitation in Remote Areas of the World, *Journal of Geophysical Research-Oceans and*
890 *Atmospheres*, 87, 8771-8786, 10.1029/JC087iC11p08771, 1982.

891 Granby, K., Egelov, A. H., Nielsen, T., and Lohse, C.: Carboxylic acids: Seasonal variation
892 and relation to chemical and meteorological parameters, *Journal of Atmospheric*
893 *Chemistry*, 28, 195-207, 10.1023/a:1005877419395, 1997.

894 Grosjean, D.: Ambient Levels of Formaldehyde, Acetaldehyde, and Formic acid in
895 Southern Californic- Results of a One-year Base-line Study, *Environmental Science &*
896 *Technology*, 25, 710-715, 10.1021/es00016a016, 1991.

897 Hansen, D. A., Edgerton, E. S., Hartsell, B. E., Jansen, J. J., Kandasamy, N., Hidy, G. M.,
898 and Blanchard, C. L.: The southeastern aerosol research and characterization study: Part 1-
899 overview, *Journal of the Air & Waste Management Association*, 53, 1460-1471, 2003.

900 Hartmann, W. R., Santana, M., Hermoso, M., Andreae, M. O., and Sanhueza, E.: Diurnal
901 Cycles of Formic and Acetic Acids in the Northern Part of the Guayana Sheld, Venezuela,
902 *Journal of Atmospheric Chemistry*, 13, 63-72, 10.1007/bf00048100, 1991.

903 Hennigan, C. J., Bergin, M. H., Russell, A. G., Nenes, A., and Weber, R. J.: Gas/particle
904 partitioning of water-soluble organic aerosol in Atlanta, *Atmos. Chem. Phys.*, 9, 3613-
905 3628, 10.5194/acp-9-3613-2009, 2009.

906 Huey, L. G., Hanson, D. R., and Howard, C. J.: Reactions of SF₆- and I- with Atmospheric
907 Trace Gases, *Journal of Physical Chemistry*, 99, 5001-5008, 10.1021/j100014a021, 1995.

908 Huey, L. G., Tanner, D. J., Slusher, D. L., Dibb, J. E., Arimoto, R., Chen, G., Davis, D.,
909 Buhr, M. P., Nowak, J. B., Mauldin, R. L., Eisele, F. L., and Kosciuch, E.: CIMS
910 measurements of HNO₃ and SO₂ at the South Pole during ISCAT 2000, *Atmospheric*
911 *Environment*, 38, 5411-5421, 10.1016/j.atmosenv.2004.04.037, 2004.

912 Kawamura, K., Ng, L. L., and Kaplan, I. R.: Determination of Organic Acids (C1-C10) in
913 the Atmosphere, Motor Exhausts, and Engine Oils, *Environmental Science & Technology*,
914 19, 1082-1086, 10.1021/es00141a010, 1985.

915 Keene, W. C., Galloway, J. N., and Holden, J. D.: Measurement of Weak Organic Acidity
916 in Precipitation from Remote Areas of the World, *Journal of Geophysical Research-Oceans*
917 *and Atmospheres*, 88, 5122-5130, 10.1029/JC088iC09p05122, 1983.

918 Keene, W. C., and Galloway, J. N.: Organic Acidity in Precipitation of North America,
919 *Atmospheric Environment*, 18, 2491-2497, 10.1016/0004-6981(84)90020-9, 1984.

920 Kesselmeier, J., Bode, K., Hofmann, U., Muller, H., Schafer, L., Wolf, A., Ciccioli, P.,
921 Brancaleoni, E., Cecinato, A., Frattoni, M., Foster, P., Ferrari, C., Jacob, V., Fugit, J. L.,
922 Dutaur, L., Simon, V., and Torres, L.: Emission of short chained organic acids, aldehydes
923 and monoterpenes from *Quercus ilex* L. and *Pinus pinea* L. in relation to physiological
924 activities, carbon budget and emission algorithms, *Atmospheric Environment*, 31, 119-133,
925 10.1016/s1352-2310(97)00079-4, 1997.

926 Kesselmeier, J.: Exchange of short-chain oxygenated volatile organic compounds (VOCs)
927 between plants and the atmosphere: A compilation of field and laboratory studies, *Journal*
928 *of Atmospheric Chemistry*, 39, 219-233, 10.1023/a:1010632302076, 2001.

929 Khare, P., Kumar, N., Kumari, K. M., and Srivastava, S. S.: Atmospheric formic and acetic
930 acids: An overview, *Reviews of Geophysics*, 37, 227-248, 10.1029/1998rg900005, 1999.

931 Kim, S., Huey, L. G., Stickel, R. E., Tanner, D. J., Crawford, J. H., Olson, J. R., Chen, G.,
932 Brune, W. H., Ren, X., Leshner, R., Wooldridge, P. J., Bertram, T. H., Perring, A., Cohen,
933 R. C., Lefter, B. L., Shetter, R. E., Avery, M., Diskin, G., and Sokolik, I.: Measurement of
934 HO₂NO₂ in the free troposphere during the intercontinental chemical transport experiment

935 - North America 2004, *Journal of Geophysical Research-Atmospheres*, 112,
936 10.1029/2006jd007676, 2007.

937 Kuhn, U., Rottenberger, S., Biesenthal, T., Ammann, C., Wolf, A., Schebeske, G., Oliva,
938 S. T., Tavares, T. M., and Kesselmeier, J.: Exchange of short-chain monocarboxylic acids
939 by vegetation at a remote tropical forest site in Amazonia, *Journal of Geophysical*
940 *Research-Atmospheres*, 107, 18, 10.1029/2000jd000303, 2002.

941 Lee, B. H., Lopez-Hilfiker, F. D., Mohr, C., Kurten, T., Worsnop, D. R., and Thornton, J.
942 A.: An Iodide-Adduct High-Resolution Time-of-Flight Chemical-Ionization Mass
943 Spectrometer: Application to Atmospheric Inorganic and Organic Compounds,
944 *Environmental Science & Technology*, 48, 6309-6317, 10.1021/es500362a, 2014.

945 Liao, J., Sihler, H., Huey, L. G., Neuman, J. A., Tanner, D. J., Friess, U., Platt, U., Flocke,
946 F. M., Orlando, J. J., Shepson, P. B., Beine, H. J., Weinheimer, A. J., Sjostedt, S. J., Nowak,
947 J. B., Knapp, D. J., Staebler, R. M., Zheng, W., Sander, R., Hall, S. R., and Ullmann, K.:
948 A comparison of Arctic BrO measurements by chemical ionization mass spectrometry and
949 long path-differential optical absorption spectroscopy, *Journal of Geophysical Research-*
950 *Atmospheres*, 116, 10.1029/2010jd014788, 2011.

951 Lide, D. R.: *CRC handbook of chemistry and physics: a ready-reference book of chemical*
952 *and physical data*, CRC Press, Boca Raton, FL, 1995.

953 Lim, H. J., Carlton, A. G., and Turpin, B. J.: Isoprene forms secondary organic aerosol
954 through cloud processing: Model simulations, *Environmental Science & Technology*, 39,
955 4441-4446, 10.1021/es048039h, 2005.

956 Millet, D. B., Baasandorj, M., Farmer, D. K., Thornton, J. A., Baumann, K., Brophy, P.,
957 Chaliyakunnel, S., de Gouw, J. A., Graus, M., Hu, L., Koss, A., Lee, B. H., Lopez-Hilfiker,
958 F. D., Neuman, J. A., Paulot, F., Peischl, J., Pollack, I. B., Ryerson, T. B., Warneke, C.,
959 Williams, B. J., and Xu, J.: A large and ubiquitous source of atmospheric formic acid,
960 *Atmos. Chem. Phys.*, 15, 6283-6304, 10.5194/acp-15-6283-2015, 2015.

961 Molina, M. J., Ivanov, A. V., Trakhtenberg, S., and Molina, L. T.: Atmospheric evolution
962 of organic aerosol, *Geophys. Res. Lett.*, 31, 10.1029/2004gl020910, 2004.

963 Nah, T., Guo, H., Sullivan, A. P., Chen, Y., Tanner, D. J., Nenes, A., Russell, A., Ng, N.
964 L., Huey, L. G., and Weber, R. J.: Characterization of Aerosol Composition, Aerosol
965 Acidity and Organic Acid Partitioning at an Agriculture-intensive Rural Southeastern U.S.
966 Site, *Atmos. Chem. Phys. Discuss.*, in review, 10.5194/acp-2018-373, 2018.

967 Neuman, J. A., Ryerson, T. B., Huey, L. G., Jakoubek, R., Nowak, J. B., Simons, C., and
968 Fehsenfeld, F. C.: Calibration and evaluation of nitric acid and ammonia permeation tubes
969 by UV optical absorption, *Environmental Science & Technology*, 37, 2975-2981,
970 10.1021/es0264221, 2003.

971 Nguyen, T. B., Crouse, J. D., Teng, A. P., Clair, J. M. S., Paulot, F., Wolfe, G. M., and
972 Wennberg, P. O.: Rapid deposition of oxidized biogenic compounds to a temperate forest,
973 *Proc. Natl. Acad. Sci. U. S. A.*, 112, E392-E401, 10.1073/pnas.1418702112, 2015.

974 Nolte, C. G., Solomon, P. A., Fall, T., Salmon, L. G., and Cass, G. R.: Seasonal and spatial
975 characteristics of formic and acetic acids concentrations in the southern California
976 atmosphere, *Environmental Science & Technology*, 31, 2547-2553, 10.1021/es960954i,
977 1997.

978 Nowak, J. B., Huey, L. G., Russell, A. G., Tian, D., Neuman, J. A., Orsini, D., Sjostedt, S.
979 J., Sullivan, A. P., Tanner, D. J., Weber, R. J., Nenes, A., Edgerton, E., and Fehsenfeld, F.
980 C.: Analysis of urban gas phase ammonia measurements from the 2002 Atlanta Aerosol
981 Nucleation and Real-Time Characterization Experiment (ANARChE), *Journal of*
982 *Geophysical Research-Atmospheres*, 111, 14, 10.1029/2006jd007113, 2006.

983 Orzechowska, G. E., and Paulson, S. E.: Photochemical sources of organic acids. 1.
984 Reaction of ozone with isoprene, propene, and 2-butenes under dry and humid conditions
985 using SPME, *J. Phys. Chem. A*, 109, 5358-5365, 10.1021/jp050166s, 2005.

986 Pan, X., Underwood, J. S., Xing, J. H., Mang, S. A., and Nizkorodov, S. A.:
987 Photodegradation of secondary organic aerosol generated from limonene oxidation by

988 ozone studied with chemical ionization mass spectrometry, *Atmos. Chem. Phys.*, 9, 3851-
989 3865, 10.5194/acp-9-3851-2009, 2009.

990 Park, J., Gomez, A. L., Walser, M. L., Lin, A., and Nizkorodov, S. A.: Ozonolysis and
991 photolysis of alkene-terminated self-assembled monolayers on quartz nanoparticles:
992 implications for photochemical aging of organic aerosol particles, *Physical Chemistry*
993 *Chemical Physics*, 8, 2506-2512, 10.1039/b602704k, 2006.

994 Paulot, F., Wunch, D., Crouse, J. D., Toon, G. C., Millet, D. B., DeCarlo, P. F.,
995 Vigouroux, C., Deutscher, N. M., Abad, G. G., Notholt, J., Warneke, T., Hannigan, J. W.,
996 Warneke, C., de Gouw, J. A., Dunlea, E. J., De Maziere, M., Griffith, D. W. T., Bernath,
997 P., Jimenez, J. L., and Wennberg, P. O.: Importance of secondary sources in the
998 atmospheric budgets of formic and acetic acids, *Atmos. Chem. Phys.*, 11, 1989-2013,
999 10.5194/acp-11-1989-2011, 2011.

1000 Seco, R., Penuelas, J., and Filella, I.: Short-chain oxygenated VOCs: Emission and uptake
1001 by plants and atmospheric sources, sinks, and concentrations, *Atmospheric Environment*,
1002 41, 2477-2499, 10.1016/j.atmosenv.2006.11.029, 2007.

1003 Sindelarova, K., Granier, C., Bouarar, I., Guenther, A., Tilmes, S., Stavrou, T., Muller,
1004 J. F., Kuhn, U., Stefani, P., and Knorr, W.: Global data set of biogenic VOC emissions
1005 calculated by the MEGAN model over the last 30 years, *Atmos. Chem. Phys.*, 14, 9317-
1006 9341, 10.5194/acp-14-9317-2014, 2014.

1007 Singh, H., Chen, Y., Tabazadeh, A., Fukui, Y., Bey, I., Yantosca, R., Jacob, D., Arnold,
1008 F., Wohlfrom, K., Atlas, E., Flocke, F., Blake, D., Blake, N., Heikes, B., Snow, J., Talbot,
1009 R., Gregory, G., Sachse, G., Vay, S., and Kondo, Y.: Distribution and fate of selected
1010 oxygenated organic species in the troposphere and lower stratosphere over the Atlantic,
1011 *Journal of Geophysical Research-Atmospheres*, 105, 3795-3805, 10.1029/1999jd900779,
1012 2000.

1013 Slusher, D. L., Pitteri, S. J., Haman, B. J., Tanner, D. J., and Huey, L. G.: A chemical
1014 ionization technique for measurement of pernitric acid in the upper troposphere and the
1015 polar boundary layer, *Geophys. Res. Lett.*, 28, 3875-3878, 10.1029/2001gl013443, 2001.

1016 Slusher, D. L., Huey, L. G., Tanner, D. J., Chen, G., Davis, D. D., Buhr, M., Nowak, J. B.,
1017 Eisele, F. L., Kosciuch, E., Mauldin, R. L., Lefer, B. L., Shetter, R. E., and Dibb, J. E.:
1018 Measurements of pernitric acid at the South Pole during ISCAT 2000, *Geophys. Res. Lett.*,
1019 29, 10.1029/2002gl015703, 2002.

1020 Sorooshian, A., Ng, N. L., Chan, A. W. H., Feingold, G., Flagan, R. C., and Seinfeld, J.
1021 H.: Particulate organic acids and overall water-soluble aerosol composition measurements
1022 from the 2006 Gulf of Mexico Atmospheric Composition and Climate Study (GoMACCS),
1023 *Journal of Geophysical Research-Atmospheres*, 112, 16, 10.1029/2007jd008537, 2007.

1024 Sorooshian, A., Murphy, S. M., Hersey, S., Bahreini, R., Jonsson, H., Flagan, R. C., and
1025 Seinfeld, J. H.: Constraining the contribution of organic acids and AMS m/z 44 to the
1026 organic aerosol budget: On the importance of meteorology, aerosol hygroscopicity, and
1027 region, *Geophys. Res. Lett.*, 37, 5, 10.1029/2010gl044951, 2010.

1028 Souza, S. R., and Carvalho, L. R. F.: Seasonality influence in the distribution of formic and
1029 acetic acids in the urban atmosphere of Sao Paulo City, Brazil, *Journal of the Brazilian*
1030 *Chemical Society*, 12, 755-762, 2001.

1031 Spaulding, R. S., Talbot, R. W., and Charles, M. J.: Optimization of a mist chamber (cofer
1032 scrubber) for sampling water-soluble organics in air, *Environmental Science &*
1033 *Technology*, 36, 1798-1808, 10.1021/es011189x, 2002.

1034 Talbot, R. W., Beecher, K. M., Harriss, R. C., and Cofer, W. R.: Atmospheric
1035 Geochemistry of Formic and Acetic Acids at a Mid-latitude Temperate Site, *Journal of*
1036 *Geophysical Research-Atmospheres*, 93, 1638-1652, 10.1029/JD093iD02p01638, 1988.

1037 Talbot, R. W., Mosher, B. W., Heikes, B. G., Jacob, D. J., Munger, J. W., Daube, B. C.,
1038 Keene, W. C., Maben, J. R., and Artz, R. S.: Carboxylic Acids in the Rural Continental
1039 Atmosphere over the Eastern United States during the Shenandoah Cloud and
1040 Photochemistry Experiment, *Journal of Geophysical Research-Atmospheres*, 100, 9335-
1041 9343, 10.1029/95jd00507, 1995.

1042 Talbot, R. W., Dibb, J. E., Scheuer, E. M., Blake, D. R., Blake, N. J., Gregory, G. L.,
1043 Sachse, G. W., Bradshaw, J. D., Sandholm, S. T., and Singh, H. B.: Influence of biomass
1044 combustion emissions on the distribution of acidic trace gases over the southern Pacific
1045 basin during austral springtime, *Journal of Geophysical Research-Atmospheres*, 104, 5623-
1046 5634, 10.1029/98jd00879, 1999.

1047 Veres, P., Roberts, J. M., Warneke, C., Welsh-Bon, D., Zahniser, M., Herndon, S., Fall, R.,
1048 and de Gouw, J.: Development of negative-ion proton-transfer chemical-ionization mass
1049 spectrometry (NI-PT-CIMS) for the measurement of gas-phase organic acids in the
1050 atmosphere, *Int. J. Mass Spectrom.*, 274, 48-55, 10.1016/j.ijms.2008.04.032, 2008.

1051 Veres, P., Roberts, J. M., Burling, I. R., Warneke, C., de Gouw, J., and Yokelson, R. J.:
1052 Measurements of gas-phase inorganic and organic acids from biomass fires by negative-
1053 ion proton-transfer chemical-ionization mass spectrometry, *Journal of Geophysical*
1054 *Research-Atmospheres*, 115, 10.1029/2010jd014033, 2010.

1055 Veres, P. R., Roberts, J. M., Cochran, A. K., Gilman, J. B., Kuster, W. C., Holloway, J. S.,
1056 Graus, M., Flynn, J., Lefer, B., Warneke, C., and de Gouw, J.: Evidence of rapid production
1057 of organic acids in an urban air mass, *Geophys. Res. Lett.*, 38, 10.1029/2011gl048420,
1058 2011.

1059 Vlasenko, A., George, I. J., and Abbatt, J. P. D.: Formation of volatile organic compounds
1060 in the heterogeneous oxidation of condensed-phase organic films by gas-phase OH, *J. Phys.*
1061 *Chem. A*, 112, 1552-1560, 10.1021/jp0772979, 2008.

1062 Walser, M. L., Park, J., Gomez, A. L., Russell, A. R., and Nizkorodov, S. A.:
1063 Photochemical aging of secondary organic aerosol particles generated from the oxidation
1064 of d-limonene, *J. Phys. Chem. A*, 111, 1907-1913, 10.1021/jp0662931, 2007.

1065 Xu, L., Guo, H. Y., Weber, R. J., and Ng, N. L.: Chemical Characterization of Water-
1066 Soluble Organic Aerosol in Contrasting Rural and Urban Environments in the Southeastern
1067 United States, *Environmental Science & Technology*, 51, 78-88, 10.1021/acs.est.6b05002,
1068 2017.

1069 Yatawelli, R. L. N., Mohr, C., Stark, H., Day, D. A., Thompson, S. L., Lopez-Hilfiker, F.
1070 D., Campuzano-Jost, P., Palm, B. B., Vogel, A. L., Hoffmann, T., Heikkinen, L., Aijala,
1071 M., Ng, N. L., Kimmel, J. R., Canagaratna, M. R., Ehn, M., Junninen, H., Cubison, M. J.,
1072 Petaja, T., Kulmala, M., Jayne, J. T., Worsnop, D. R., and Jimenez, J. L.: Estimating the
1073 contribution of organic acids to northern hemispheric continental organic aerosol,
1074 *Geophys. Res. Lett.*, 42, 6084-6090, 10.1002/2015gl064650, 2015.

1075 Zhang, R. Y., Suh, I., Zhao, J., Zhang, D., Fortner, E. C., Tie, X. X., Molina, L. T., and
1076 Molina, M. J.: Atmospheric new particle formation enhanced by organic acids, *Science*,
1077 304, 1487-1490, 10.1126/science.1095139, 2004.

1078

1079

1080

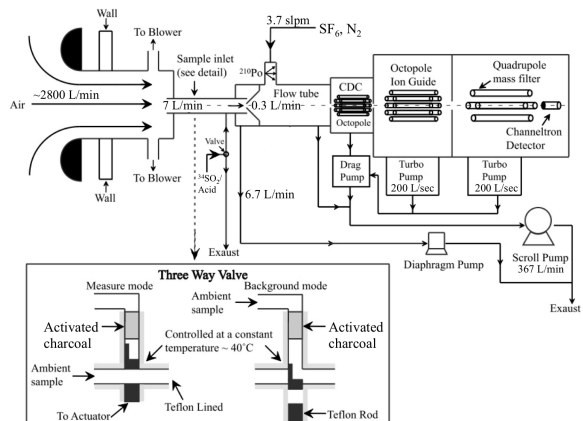
1081

1082

1083

1084

1085



1086

1087 **Figure 1:** The CIMS instrument and inlet configuration used in the field study. The
 1088 automated three-way sampling valve is shown in the inset. The figure was adapted from
 1089 Liao et al. (2011).

1090

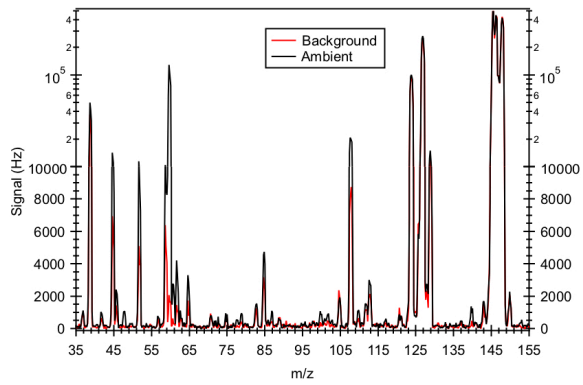
1091

1092

1093

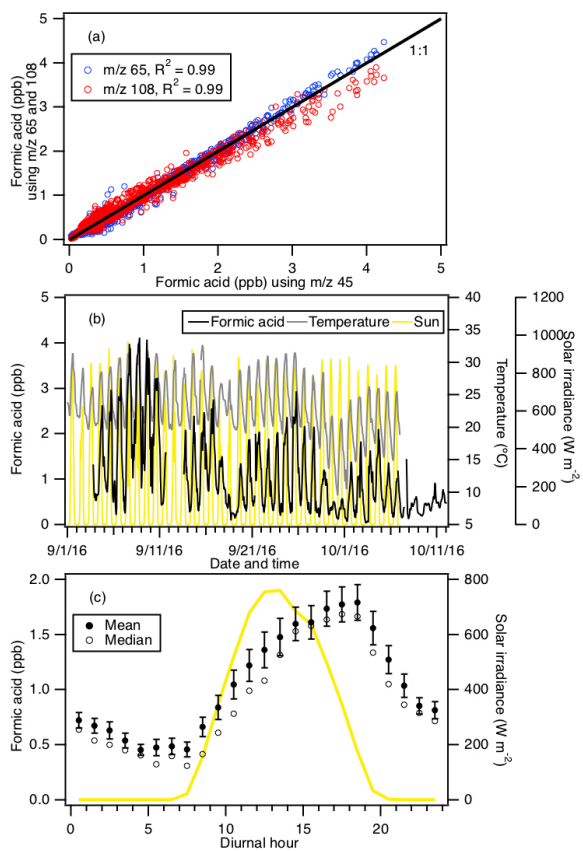
1094

1095



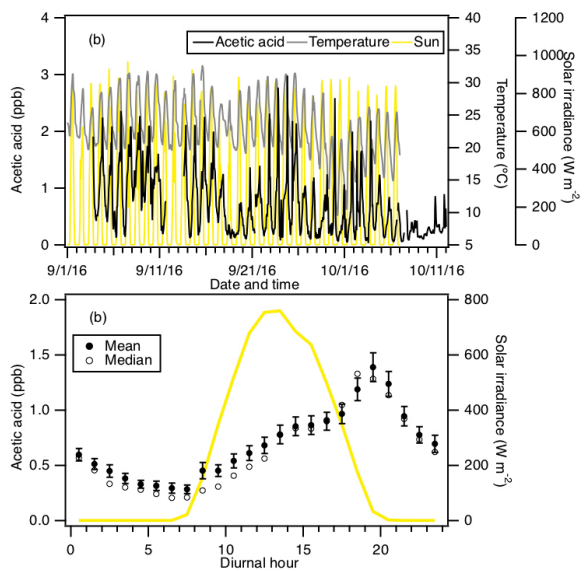
1096

1097 **Figure 2:** Mass spectrum of ambient air and background measured in Yorkville, Georgia
 1098 on 8 Sept 2016 using SF₆⁻. Note that the ³²SF₆⁻ reagent ion signal (at m/z 146) is saturated,
 1099 causing the sharp drop in its signal. As a result, the ion signal of its isotope ³⁴SF₆⁻ (at m/z
 1100 150) was monitored to determine if the reaction of SF₆⁻ with ambient water vapor and O₃
 1101 depleted SF₆⁻ reagent ions.



1102

1103 **Figure 3:** (a) Scatter plot comparison of ambient formic acid concentrations determined
 1104 using mass peaks m/z 45, 65 and 108. The three datasets correlated well with one another
 1105 ($R^2 = 0.99$). Linear regression of the data gave slopes of 1 (for m/z 65) and 0.95 (for m/z
 1106 108), indicating that all three mass peaks can be used to determine the formic acid
 1107 concentration. (b) Time series of formic acid concentration, temperature and solar
 1108 irradiance. All the data are displayed as 1-hour averages. (c) Diurnal profiles of formic acid
 1109 concentration (symbols) and solar irradiance (yellow line). All the concentrations represent
 1110 averages in 1-hour intervals and the standard errors are plotted as error bars.



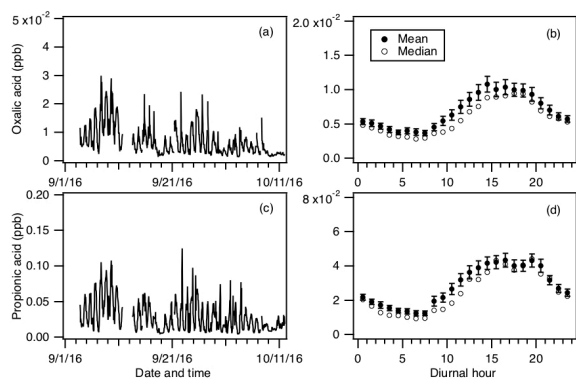
1111

1112 **Figure 4:** (a) Time series of acetic acid concentration, temperature and solar irradiance.
 1113 All the data are displayed as 1-hour averages. (c) Diurnal profiles of acetic acid (symbols)
 1114 and solar irradiance (yellow line). All the concentrations represent averages in 1-hour
 1115 intervals and the standard errors are plotted as error bars.

1116

1117

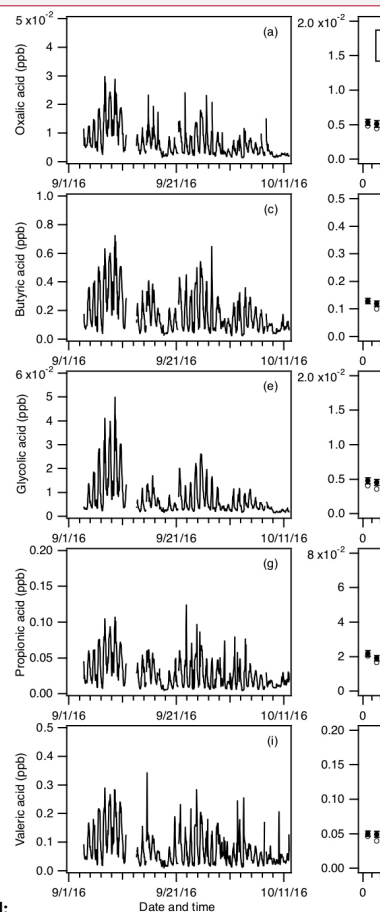
1118



Formatted: Centered

1119

1120 **Figure 5:** Time series of concentrations of (a) oxalic and (c) propionic acids measured
 1121 during the field study. All the data are displayed as 1-hour averages. Their corresponding
 1122 diurnal profiles are shown in (b) and (d), respectively. The diurnal profile concentrations
 1123 represent averages in 1-hour intervals and the standard errors are plotted as error bars.



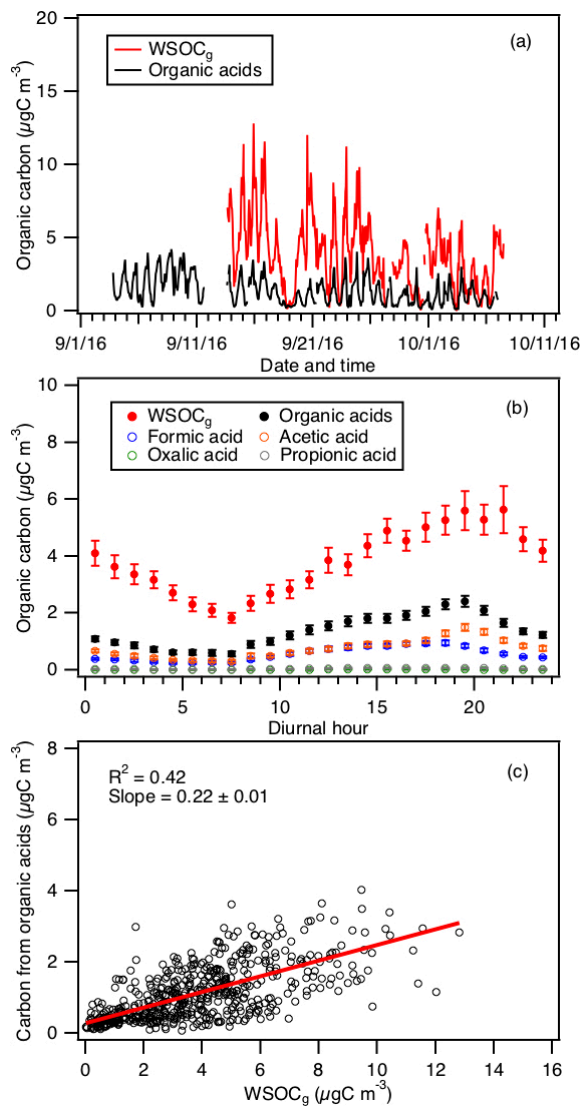
Deleted:

Deleted: ,

Deleted: (c) butyric, (e) glycolic, (g) propionic, and (i) valeric acids

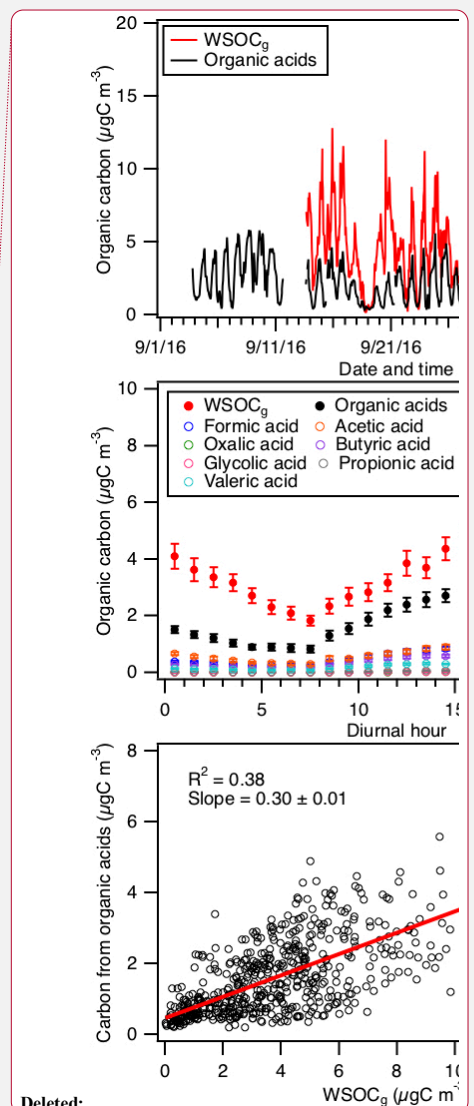
Deleted: ,

Deleted: (f), (h) and (j),



1130

1131 **Figure 6:** (a) Time series of $WSOC_g$ and the total organic carbon contributed by formic,
 1132 acetic, oxalic and propionic acids. All the data are displayed as 1-hour averages. (b) Diurnal
 1133 profiles of $WSOC_g$ and the total organic carbon contributed by formic, acetic, oxalic and

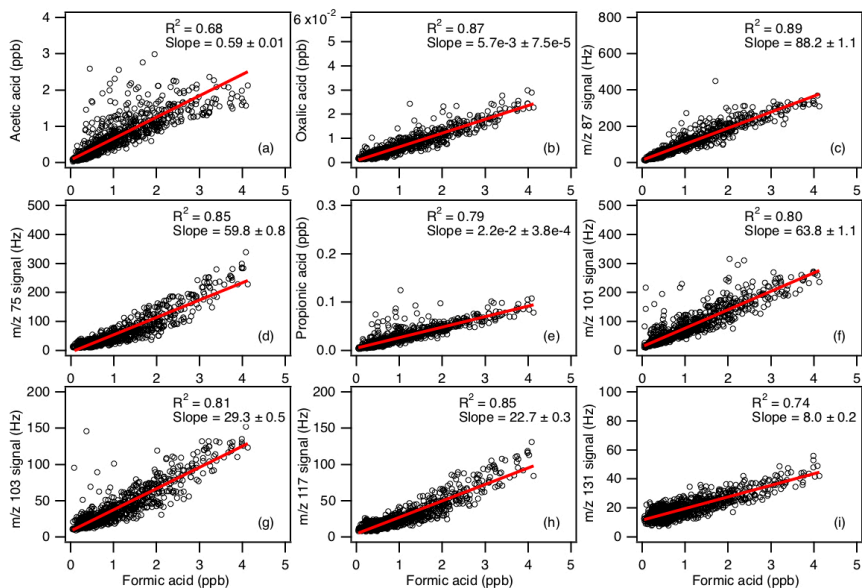


Deleted:

Deleted: the measured organic

Deleted: the measured

1137 propionic acids. Also shown are the diurnal profiles of the organic carbon contributed by
 1138 the individual organic acids. All the concentrations represent the mean hourly averages and
 1139 the standard errors are plotted as error bars. (c) Scatter plot of total organic carbon
 1140 contributed by formic, acetic, oxalic and propionic acids with WSOC_g.



1141
 1142 **Figure 7:** Scatter plots of concentrations (or ion signals) of the measured organic acids
 1143 with formic acid concentration. All the data are displayed as 1-hour averages. Red lines
 1144 shown are linear fits to the data.

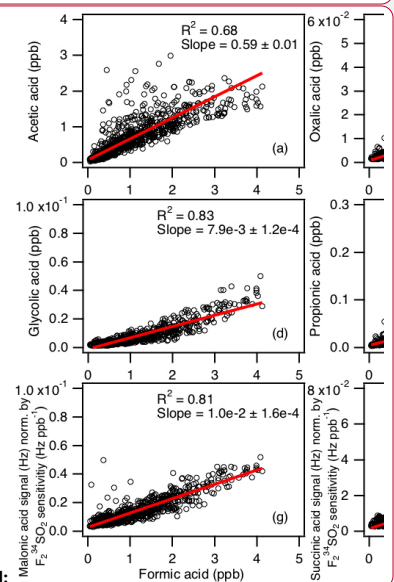
~~Deleted:~~ organic

~~Deleted:~~ measured

~~Deleted:~~ the measured organic

~~Deleted:~~ Note that the ion peak assignment to some of these organic acids are speculative.

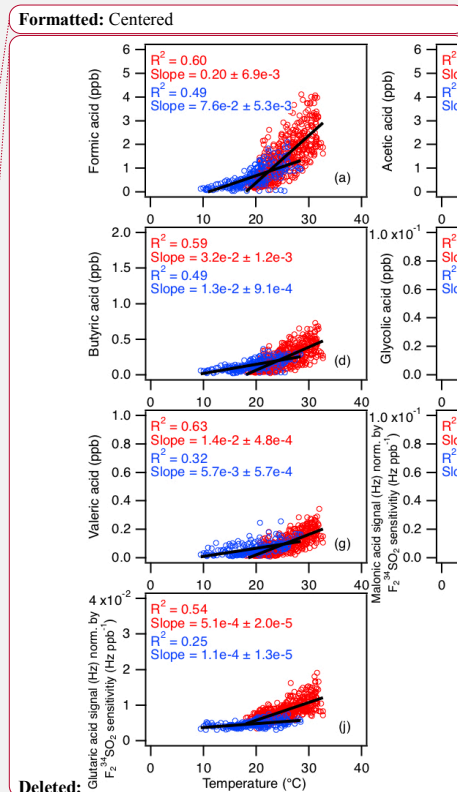
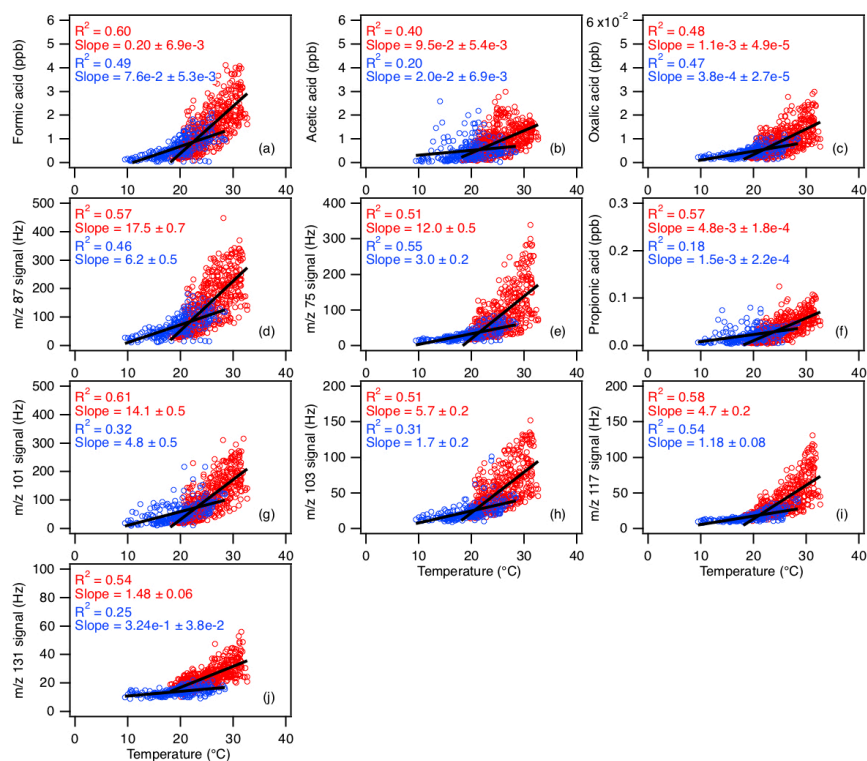
Formatted: Centered



~~Deleted:~~

~~Deleted:~~ (a) acetic, (b) oxalic, (c) butyric, (d) glycolic, (e) propionic, (f) valeric, (g) malonic, (h) succinic, and (i) glutaric acids

~~Deleted:~~ The data for malonic, succinic and glutaric acids are presented as the ratio of their ion signals (Hz) to the instrument's sensitivity to $F_2^{34}SO_2$ ($Hz\ ppb^{-1}$) since these organic acids were not calibrated.



Deleted: (a) formic, (b) acetic, (c) oxalic, (d) butyric, (e) glycolic, (f) propionic, (g) valeric, (h) malonic, (i) succinic, and (j) glutaric acids

Deleted: The data for malonic, succinic and glutaric acids are presented as the ratio of their ion signals (Hz) to the instrument's sensitivity to $F_2^{34}SO_2$ (Hz ppb⁻¹) since these organic acids were not calibrated.

1158
1159
1160
1161
1162
1163
1164
1165
1166
1167

1176 **Table 1:** Summary of organic acids of interest, their detection limits and sensitivities of
 1177 their X⁻ and X⁻•HF ions^a

Organic Acid	Detection limit (ppt) ^b	Sensitivity (Hz ppt ⁻¹)	
		X ⁻	X ⁻ •HF
Formic acid	30	1.29 ± 0.22	0.29 ± 0.05
Acetic acid	60	1.46 ± 0.29	0.30 ± 0.06
Oxalic acid	1	6.38 ± 0.32	0.97 ± 0.05
Butyric acid	30	0.41 ± 0.01	0.12 ± 0.004
Glycolic acid	2	5.53 ± 0.11	1.64 ± 0.03
Propionic acid	6	2.05 ± 0.02	1.26 ± 0.01
Valeric acid	10	0.76 ± 0.008	0.35 ± 0.004

1178 ^aOnly organic acids with calibration measurements are shown.

1179 ^bDetection limits are approximated from 3 times the standard deviation values (3σ) of the
 1180 ion signals measured during background mode. Shown here are the average detection limits
 1181 of the organic acids for 2.5 min averaging periods which corresponds to the length of a
 1182 background measurement at a 4 % duty cycle for each mass.

1 **Supplementary Information:**

2 **Real-time measurements of gas-phase organic acids using SF₆⁻ chemical ionization**
3 **mass spectrometry**

4
5 Theodora Nah,^{1,a} Yi Ji,^{1,2} David J. Tanner,¹ Hongyu Guo,¹ Amy P. Sullivan,³ Nga Lee
6 Ng,^{1,2} Rodney J. Weber¹ and L. Gregory Huey^{1*}

7
8 ¹*School of Earth and Atmospheric Sciences, Georgia Institute of Technology, Atlanta, GA, USA*

9 ²*School of Chemical and Biomolecular Engineering, Georgia Institute of Technology, Atlanta, GA, USA*

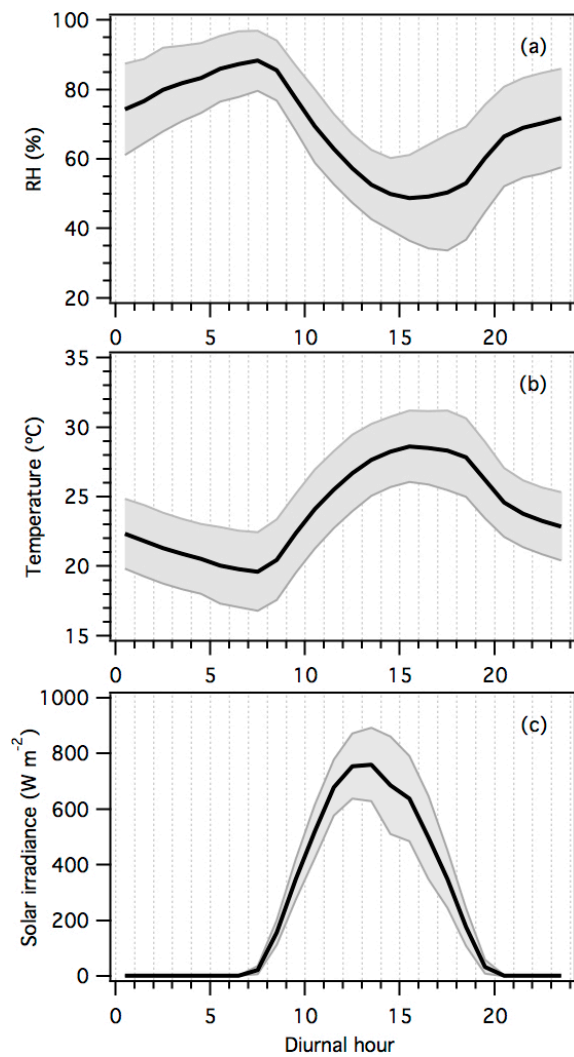
10 ³*Department of Atmospheric Science, Colorado State University, Fort Collins, CO, USA*

11 ^a*Now at School of Energy and Environment, City University of Hong Kong, Kowloon, Hong Kong, China*

12 * *To whom correspondence should be addressed: greg.huey@eas.gatech.edu*

Formatted: Line spacing: single

Deleted: ¶

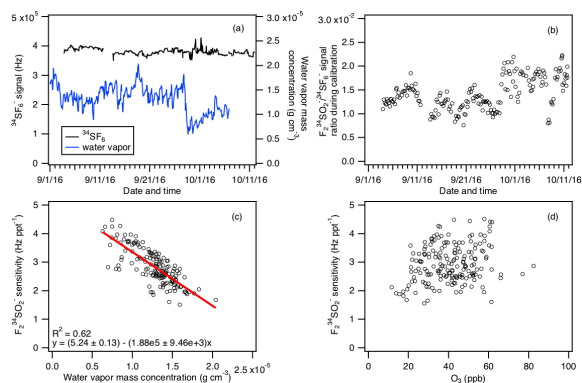


14

15 **Figure S1:** Diurnal trends of (a) relative humidity, (b) temperature, and (c) solar radiance.

16 The lines within the shaded area represents the average values. The upper and lower

17 boundaries of the shaded areas mark one standard deviation.



18

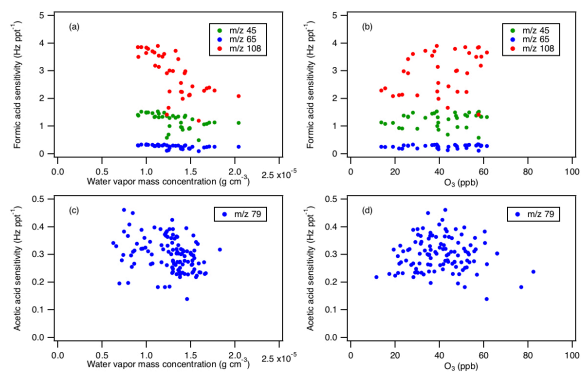
19 **Figure S2:** (a) Time series of ³⁴SF₆⁻ reagent ion signal and ambient water vapor
 20 concentration for the entire field study. The ambient water vapor mass concentrations are
 21 determined from ambient relative humidities and temperatures. (b) Time series of F₂³⁴SO₂⁻
 22 /³⁴SF₆⁻ ion signal ratio obtained during calibration measurements. Panels (c) and (d) show
 23 the F₂³⁴SO₂⁻ ion sensitivity obtained from calibration measurements as a function of
 24 ambient water vapor and O₃ concentrations. Data in panels (a) to (d) are displayed as 1-
 25 hour averages.

26

27

28

29



30

31 **Figure S3:** Panels (a) and (b) show the sensitivities of formic acid ions (HCOO⁻ at m/z 45,
 32 HCOO⁻•HF at m/z 65, and SF₄⁻ at m/z 108) obtained from calibration measurements as a
 33 function of ambient water vapor and O₃ concentrations. Panels (c) and (d) show the acetic
 34 acid sensitivity (CH₃COO⁻•HF at m/z 79) obtained from calibration measurements as a
 35 function of ambient water vapor and O₃ concentrations.

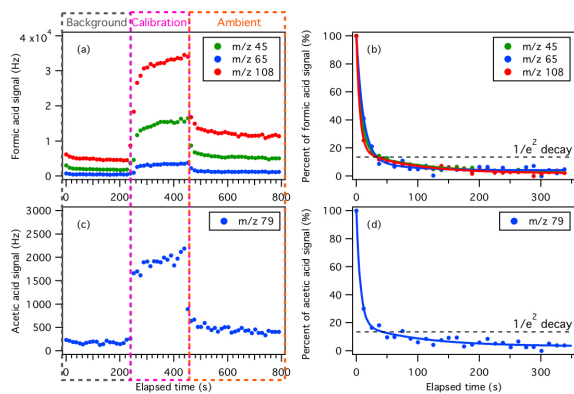
36

37

38

39

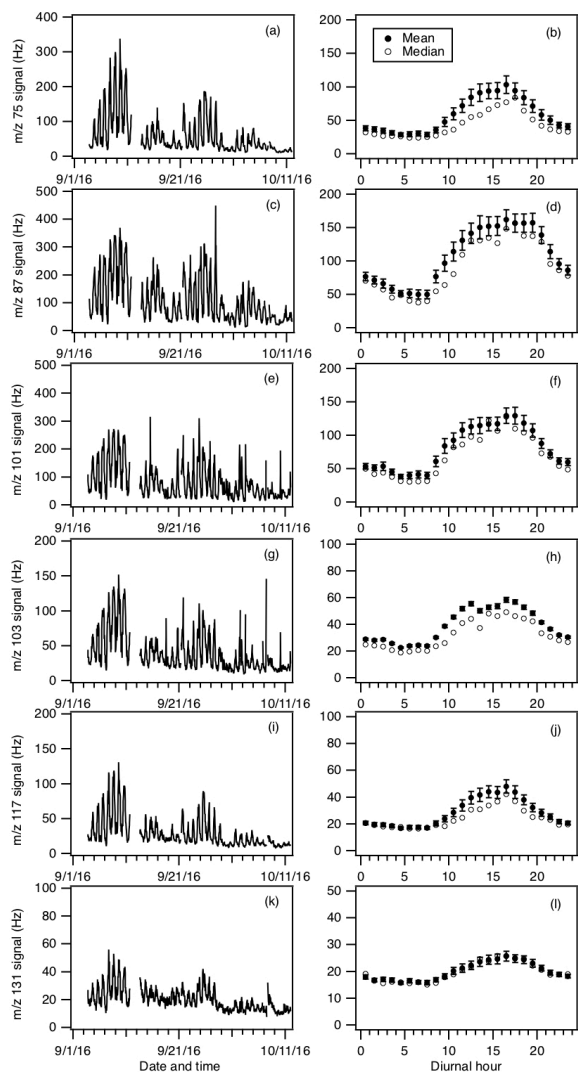
40



41

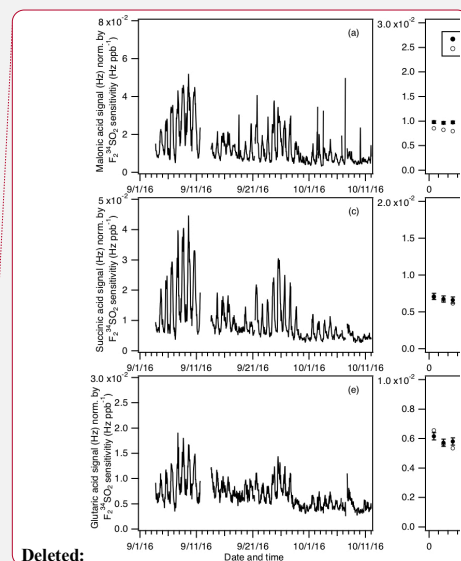
42 **Figure S4:** Example of the CIMS instrument response during switches between
 43 background, calibration and ambient measurements of (a) formic, and (c) acetic acids.
 44 Panels (b) and (d) show the percent of formic and acetic acid ion signals after the removal
 45 of a 6.75 ppb of formic acid and 5.87 ppb of acetic acid standard addition calibration as a
 46 function of time. The data shown here is 13 s time resolution data. Double exponential fits
 47 to each m/z ion are shown as colored solid lines. Black dashed lines show the times for the
 48 ions to decay to $1/e^2$.

49



50

51 **Figure S5:** Time series and diurnal profiles of ion signals of organic acids with m/z 75, 87,
 52 101, 103, 117 and 131 measured during the field study. The data are displayed as 1-hour
 53 averages. All the signals represent averages in 1-hour intervals and the standard errors are
 54 plotted as error bars.

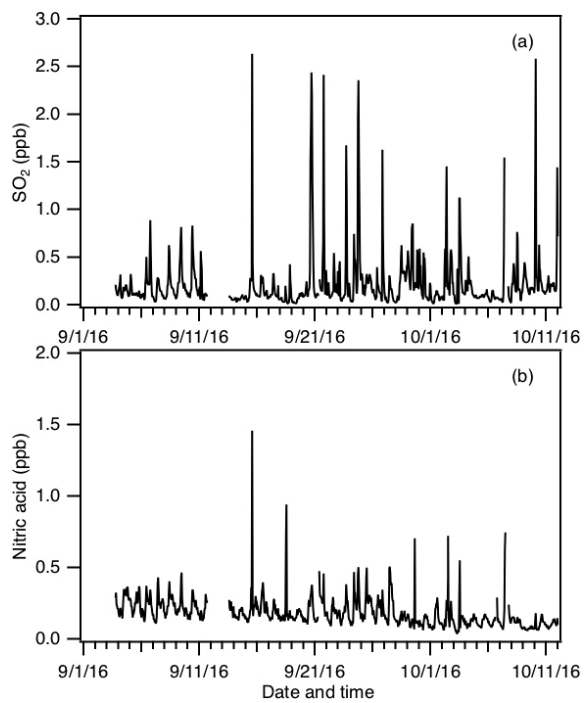


Deleted:

Deleted: (a) malonic, (c) succinic, and (e) glutaric

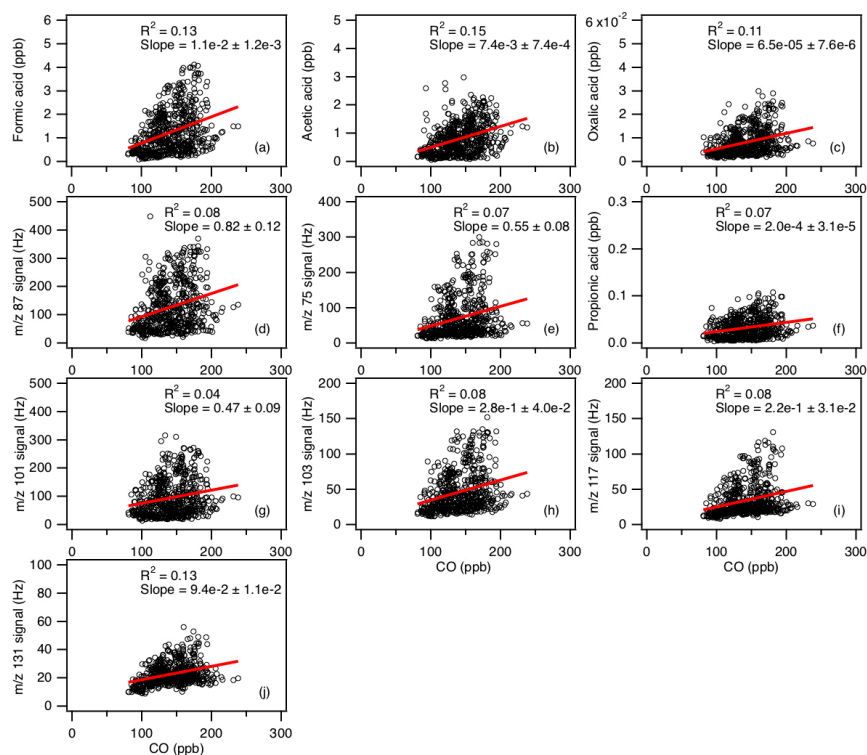
Deleted: Their corresponding diurnal profiles are shown in (b), (d) and (f), respectively.

Deleted: These organic acids were not calibrated so all the signals are presented here as Hz normalized by the instrument's sensitivity to $F_2^{34}SO_2$ ($Hz\ ppb^{-1}$) which was the primary calibrant used in the field study.



63

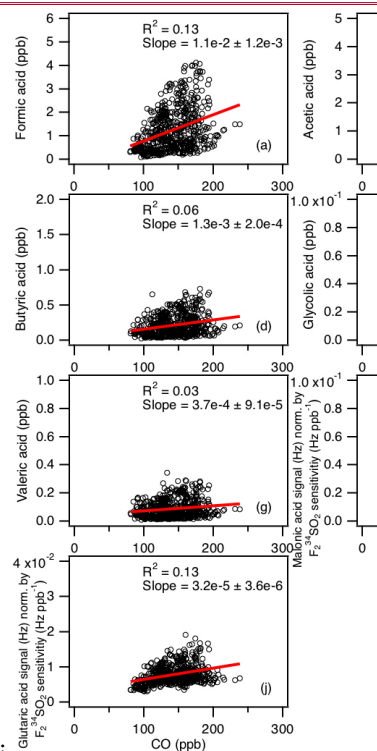
64 **Figure S6:** Time series of (a) SO₂ and (b) HNO₃ concentrations measured during the field
65 study. All the data are displayed as 1-hour averages.



66

67 **Figure S7:** Scatter plots of concentrations (or ion signals) of the measured organic acids
 68 with CO concentration. All the data are displayed as 1-hour averages. Red lines shown are
 69 linear fits to the data.

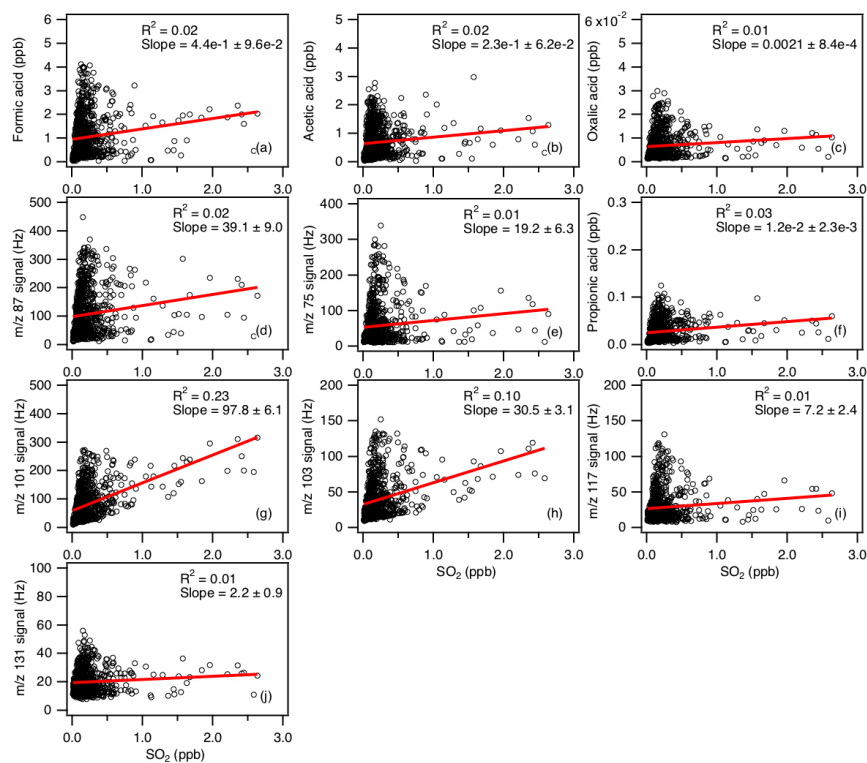
Formatted: Centered



Deleted:

Deleted: (a) formic, (b) acetic, (c) oxalic, (d) butyric, (e) glycolic, (f) propionic, (g) valeric, (h) malonic, (i) succinic, and (j) glutaric

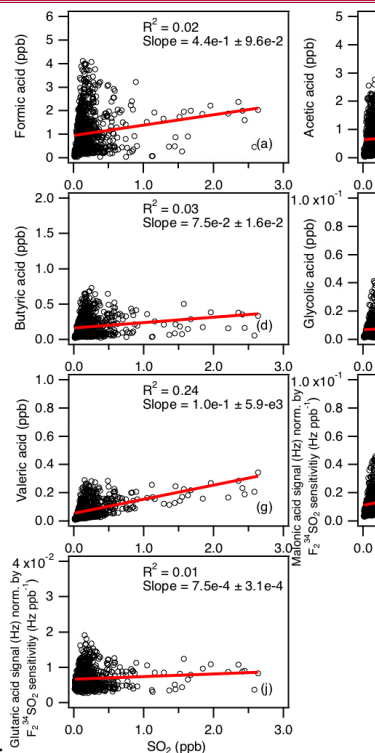
Deleted: The data for malonic, succinic and glutaric acids are presented as the ratio of their ion signals (Hz) to the instrument's sensitivity to $F_2^{34}SO_2$ ($Hz\ ppb^{-1}$) since these organic acids were not calibrated.



78

79 **Figure S8:** Scatter plots of concentrations (or ion signals) of the measured organic acids
 80 with SO₂ concentration. All the data are displayed as 1-hour averages. Red lines shown are
 81 linear fits to the data.

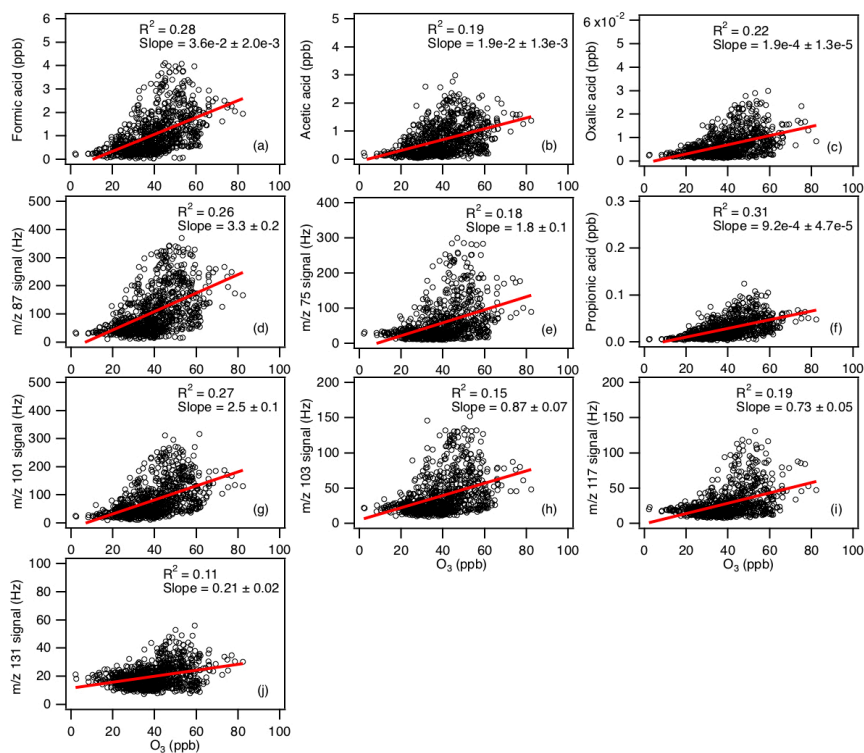
Formatted: Centered



Deleted:

Deleted: (a) formic, (b) acetic, (c) oxalic, (d) butyric, (e) glycolic, (f) propionic, (g) valeric, (h) malonic, (i) succinic, and (j) glutaric

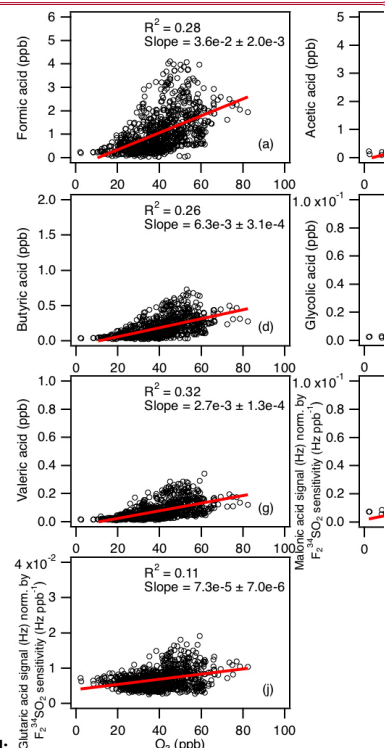
Deleted: The data for malonic, succinic and glutaric acids are presented as the ratio of their ion signals (Hz) to the instrument's sensitivity to F₂³⁴SO₂ (Hz ppb⁻¹) since these organic acids were not calibrated.



90

91 **Figure S9:** Scatter plots of concentrations (or ion signals) of the measured organic acids
 92 with O₃ concentration. All the data are displayed as 1-hour averages. Red lines shown are
 93 linear fits to the data.

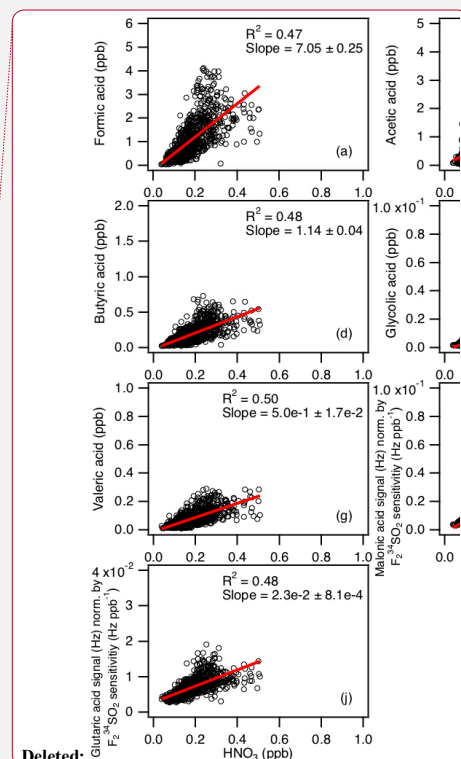
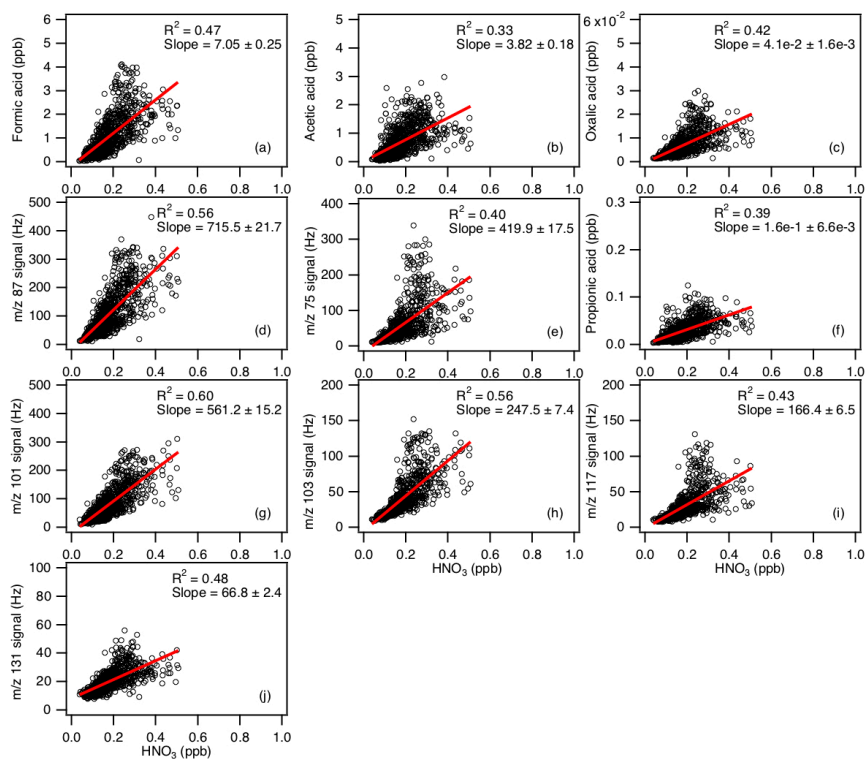
Formatted: Centered



Deleted:

Deleted: (a) formic, (b) acetic, (c) oxalic, (d) butyric, (e) glycolic, (f) propionic, (g) valeric, (h) malonic, (i) succinic, and (j) glutaric

Deleted: The data for malonic, succinic and glutaric acids are presented as the ratio of their ion signals (Hz) to the instrument's sensitivity to F₂³⁴SO₂ (Hz ppb⁻¹) since these organic acids were not calibrated.



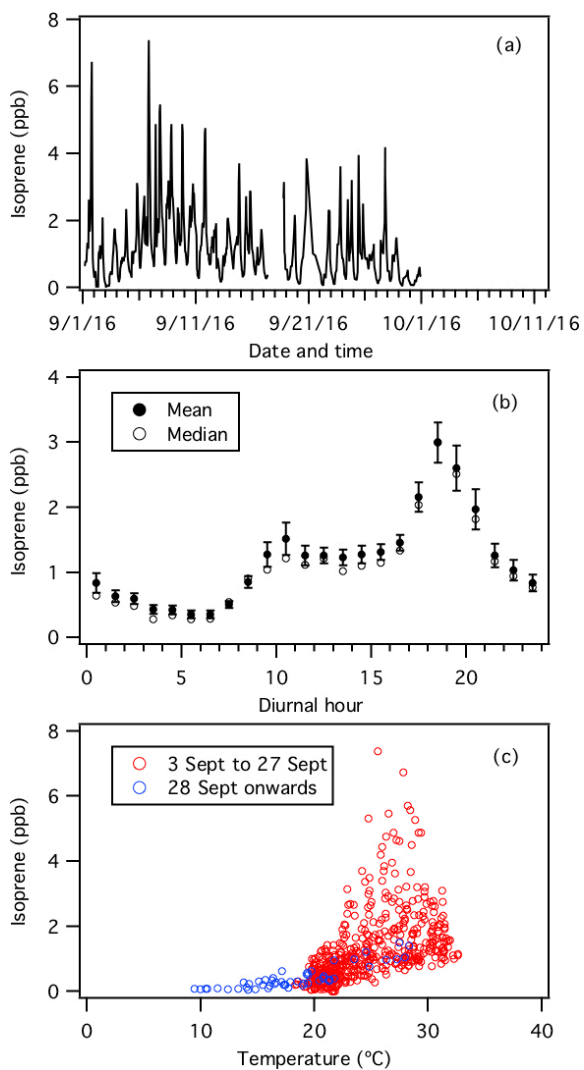
Deleted:

Deleted: (a) formic, (b) acetic, (c) oxalic, (d) butyric, (e) glycolic, (f) propionic, (g) valeric, (h) malonic, (i) succinic, and (j) glutaric

Deleted: The data for malonic, succinic and glutaric acids are presented as the ratio of their ion signals (Hz) to the instrument's sensitivity to $F_2^{34}SO_2$ ($Hz\ ppb^{-1}$) since these organic acids were not calibrated.

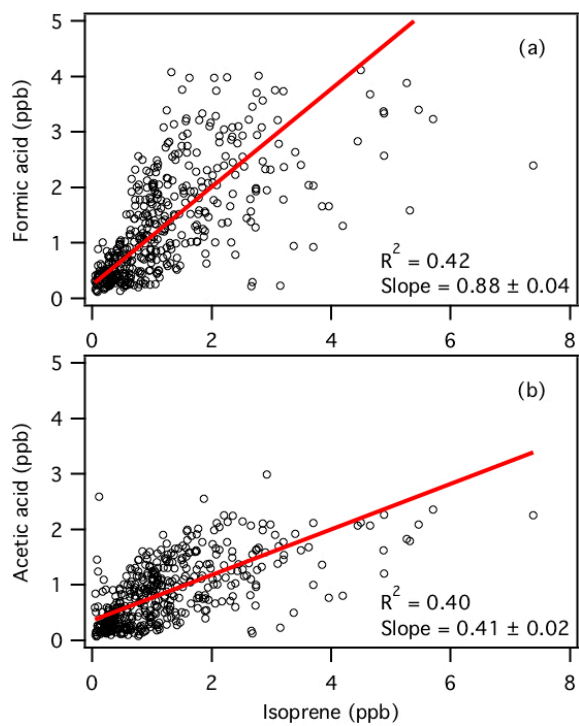
102

103 **Figure S10:** Scatter plots of concentrations (or ion signals) of the measured organic acids
 104 with HNO_3 concentration. To exclude periods when the site was affected by urban or power
 105 plant emissions, data where $HNO_3 > 0.5$ ppb are excluded from these scatter plots. All the
 106 data are displayed as 1-hour averages. Red lines shown are linear fits to the data.



115

116 **Figure S11:** (a) Time series of isoprene concentration during the field study. (b) Diurnal
 117 profile of isoprene. All the concentrations represent averages in 1-hour intervals and the
 118 standard errors are plotted as error bars. (c) Scatter plot of isoprene concentration with
 119 ambient temperature. All the data are displayed as 1-hour averages.



120

121 **Figure S12:** Scatter plots of concentrations of (a) formic and (b) acetic acids with isoprene
122 concentration. All the data are displayed as 1-hour averages. Red lines shown are linear
123 fits to the data.